Biogeochemistry and biomineralogy

Belskaya L.V., Golovanova O.A. Experimental study of the parameters of human saliva as a mineral-forming medium

Omsk State University, Omsk LudaB2005@mail.ru

Research conducted in the normal saliva and dental calculus formation. It is shown that changing the chemical composition of saliva creates conditions favorable for the formation of hydroxyapatite. Features of the elemental composition of saliva in lithogenesis in an oral cavity were installed.

Key words: pathogenic mineralization, saliva, dental calculus, chemical composition, the experiment, trace elements

Reference: Belskaya, L. V., O. A. Golovanova (2012), Experimental study of the parameters of human saliva as a mineral-forming medium, *Vestnik ONZ RAS, 4,*

Calculi formation in an oral cavity is a fairly common disease, the causes of which are currently not well established. Several authors point to the important role of saliva in the formation of dental calculus [*Borowski, 1991; Galiulina, 1988, 2000; Leontiev, 1991*].

The normal composition of saliva is well understood. However, studies of saliva composition in conditions of calculi formation in an oral cavity are rare. It is interesting to determine the content of macro-and microelements in normal human saliva, as well as in terms of calculi formation in an oral cavity, and to identify features of the environment of dental calculus formation. Therefore, the aim of this study was to determine the basic parameters of saliva in normal conditions and calculi formation.

Materials and Methods. The material used in the study was supernatant saliva of people with dental plaque and the healthy, selected as the control group (a total of 250 samples). Saliva was collected in the morning on an empty stomach before brushing teeth, centrifuged at 3000 rev / min. The following parameters were determined in all samples of saliva: pH, pK, pNa, the concentration of calcium, phosphorus, protein, and type of microcrystallization. Such parameters as pH, pK, pNa were measured by direct potentiometry using ion-selective electrodes. Protein was determined photometrically by the method of Benedict. Inorganic phosphorus in the saliva were determined by the method of Leontiev V.K. [Leontiev, 1976], the total concentration of calcium – by complexometric titration. Mathematical data processing was carried out using the statistical package STATISTICA 6.0 (Stat Soft Inc. USA).

The elemental composition of the saliva samples was determined by atomic emission spectroscopy with inductively coupled plasma (ICP-AES). The measurements were made on the spectrometer OPTIMA 2000 DV (Perkin Elmer, Germany). Processing of the results was performed using the software of the spectrometer. The method of calibration curve is used for a quantitative calculation.

Results and discussion. Previously, using XRD and IR spectroscopy [*Belskaya, 2009*] was established that the mineral component of dental calculus inhabitants of Omsk represented carbonate-containing hydroxyapatite, as an impurity found brushite (5–10%). It is known that brushite crystallizes at lower pH than the apatite [*Belskaya, 2008*]. The presence of brushite and apatite in one sample shows significant variations in the saliva pH in the process of formation and growth of dental calculus.

The research of samples by the method of XRF-SR was conducted to identify and quantify the content of the maximum possible number of trace elements in dental calculus [*Golovanova, 2006*]. All the samples revealed the presence of 29 trace elements, whose content varies in a fairly wide range from 10^{-4} to 10^{-2} wt.% (Table 1).

On the content of the elements defined in the dental calculus, can be divided into three groups:

1) containing $10^{-3} \div 10^{-2}$ wt.% - Ti, V, Cr, Mn, Fe, Ni, Cu, Zn, Br, Sr, Ba.
2) containing $10^{-4} \div 10^{-3}$ wt.% – Ga, Rb, Zr, Mo, Ag, Sn, I, La, Ce.
3) containing $< 10^{-4}$ wt.% – As, Se, Y, Nb, Cd, In, Sb, Te, Cs.

All these elements are essential, ie, vital. The wide range of individual fluctuations in the content of the elements determined, apparently, the balance of trace elements and features of the metabolic processes in the human body.

Table 1. Trace element composition of dental calculus according to XRF-SR, $\cdot 10^{-4}$ wt.%

Element	Range of the individual fluctuations	Mean value	Element	Range of the individual fluctuations	Mean value
Ti	5.8–226.9	76.2	Zr	0.3–74.9	3.6
V	7.4–117.5	42.7	Nb	0.50–1.30	0.90
Cr	17.3–319.5	70.6	Mo	0.3–4.9	1.39
Mn	7.0–45.6	24.1	Ag	0.35–6.00	2.08
Fe	1.4–417.5	81.9	Cd	0.3–1.0	0.63
Ni	1.0–47.1	16.0	In	0.313–0.794	0.532
Cu	1.7–74.4	15.3	Sn	0.3–4.4	1.5
Zn	1.0–880.9	251.9	Sb	0.3–2.6	0.6
Ga	0.3–11.7	3.0	Te	0.27–2.10	1.0
As	0.26–5.10	0.84	I	0.5–34.0	4.4
Se	0.3–1.4	0.87	Cs	0.6–1.4	0.96
Br	0.6–816.9	34.7	Ba	5.2–312.0	40.9
Rb	0.3–11.2	1.35	La	0.6–16.0	7.6
Sr	37.9–177.3	88.2	Ce	0.3–333.6	30.1
Y	0.27–2.10	0,87			-

We can assume that most of the elements in the first group included of the crystal structure of apatite isomorphic to: Sr, Ba – in the position of Ca; Ti, V, Cr – in the tetrahedral position of P. In addition, since most identified in this group elements (Zn, Cu, Ni, Fe, etc.) are good complexing agents, they can form stable complexes with the organic component of the calculus. The elements of the second and third groups received the body mainly through food and accumulate in the calculi due to their ability to concentrate in the bone tissue, particularly in the areas of growth (eg, Ga, Sn, etc.).

The next phase was investigated the chemical composition of the saliva of patients with dental calculus. It is shown that under conditions of calculi formation in an oral cavity is a shift of pH to the alkaline side (table 2). It is at these pH values are optimal conditions for the formation of hydroxyapatite – the main mineral component of human dental calculus [*Belskaya, 2009*]. Simultaneously, the total mineralization (the concentration of ions of phosphorus, sodium, potassium) increased, but decreased the protein content.

Table 2. Comparative characteristics of the saliva of people with different oral health

Rate	Control group n=47; t=1,96	Dental calculus n=31; t=1,96
pH	6.80±0.11	7.04±0.12
C (Na), g / l	0.30±0.04	0.38±0.08
C (K), g / l	0.72±0.05	1.15±0.13
Total calcium, g / l	0.051±0.004	0.055±0.005
Phosphorus, g / l	0.16±0.01	0.20±0.02
Protein, g / l	1.73±0.24	1.39±0.39

It is known that saliva is a structured biological fluid, the entire volume is distributed between the micelles – colloid formation [*Leontiev, 1991*]. Their nuclei are composed of calcium phosphate molecules and are surrounded by water and protein membranes.

$\{[m(Ca_3(PO_4)_2]s\ nHPO_4^{2-}(n-x)Ca^{2+}\}^{2x-}xCa^{2+}$

Alkalization of saliva, contributing to higher of PO_4^{3-} ions content leads to a change in the composition of the micelles and their destruction (fig. 1):

$\{[mCa_3(PO_4)_2]\ nPO_4^{3-}3/2(n-x)/2Ca^{2+}\}^{3x}\ 3/2\ xCa^{2+}$

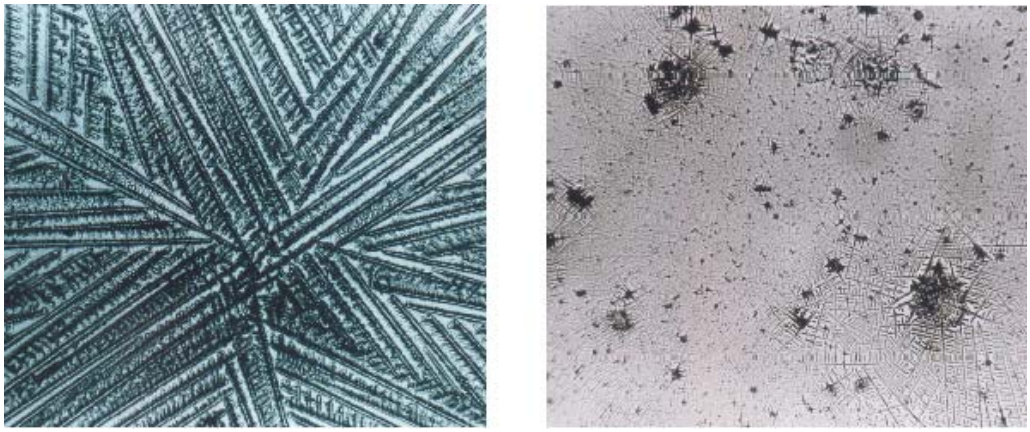

Fig. 1. Violation of the structural properties of saliva in the formation of calculi

Table 3. Characteristics of trace element composition of saliva, mg / l

Element	Control group	Dental calculus
Zn	0.476±0.183	1.082±1.010
Cu	0.342±0.314	0.054±0.033
Fe	0.278±0.041	0.399±0.185
Mn	0.050±0.014	-
Al	0.705±0.094	-

Upset micellization process due to the fact that the ions Ca^{2+} and HPO_4^{2-}, cannot simultaneously be in the adsorbed layer, since it is formed a law soluble compound $Ca_3(PO_4)_2$. In this case, with the participation of microorganisms, exciting the precipitated particles $Ca_3(PO_4)_2$ and transferring them to the rough surface of the enamel, creating favorable conditions for the formation of calculi.

Using ICP-AES revealed that the content of zinc and iron increases in saliva in calculi formation (Table 3).

The correlation analysis was made in order to establish the correlation between composition of dental calculus and saliva. In those experiments, n = 10, significance level of f = 0.01, confidence level of P = 0.99 presence of linear correlation was considered proven if the correlation coefficient in excess of the value of r = 0.65 (Table 4).

As can be seen from these data, there is a positive correlation between the viscosity of saliva and bromine, it can be explained by the fact that bromine is more accumulated in the organic component of dental calculus, and organic matter content, in turn, correlates with the viscosity of saliva.

Relatively high values of correlation coefficients of calcium and phosphorus in the saliva, as well as barium and strontium in the composition of dental calculus, can be explained by the proximity of the ionic radii of these elements ($r(Ca^{2+})$ = 0.100±0.003, $r(Ba^{2+})$ = 0.137±0.005, $r(Sr^{2+})$ = 0.116±0.003 nm) and the ability to isomorphic substitution in the crystal structure of hydroxyapatite – the main mineral component of human dental calculus. Similar patterns are revealed for potassium in the saliva and the ions of iron, zinc, nickel and vanadium in the composition of dental calculus. Since potassium ions are in the hydration shell of the micelles of calcium phosphate, in the process of formation and growth of calculus may be substituted by ions coming into the oral cavity, and the concentration of potassium ions in the saliva with the natural increase.

Table 4. The correlation coefficients between the parameters of the composition of saliva and dental calculus

The parameters of saliva	The composition of dental calculus
pH	V (r = -0.69), Fe (r = -0.68), Ni (r = -0.68), **Ag (r = 0.68)**
Viscosity	**Br (r = 0.75)**
Potassium	**V (r = 0.72), Fe (r = 0.71), Ni (r = 0.71), Zn (r = 0.66),** Ag (r = -0.66)
Calcium	**Ba (r = 0.78)**, Mn (r = -0.82), Rb (r = -0.68), Ag (r = -0.68)
Phosphorus	Br (r = -0.73), Rb (r = -0.88), Ag (r = -0.88), **Sr (r = 0.74), Ba (r = 0.65)**
Ca/P	Mn (r = -0.93), **I (r = 0.68)**
Na/K	**Rb (r = 0.66), Ag (r = 0.89)**

The negative correlation between the content of vanadium ions, iron and nickel in the composition of dental calculus, and the pH of saliva due to the fact that with increasing pH the predominant form of existence of these ions in solution is anionic and the ability to isomorphic substitution decreases.

Conclusion. Based on the experimental data can distinguish the changes occurring in the saliva of a person in calculi formation in the oral cavity:

1. Under the conditions of calculi formation in the oral cavity is a shift of pH to the alkaline side, which creates favorable conditions for the formation of hydroxyapatite.
2. In the formation of dental calculus in saliva decreased the content of calcium ions, but increases the content of phosphorus and electrolyte components – sodium and potassium ions.
3. A decrease in protein content in the saliva of patients with dental calculi, indicating that violation of the structural properties of saliva.
4. It was established that under conditions of calculi formation in the mouth increases the content of zinc and iron.

References:

1. Belskaya, L. V. (2009). Dental and salivary stones – the chemical composition, genetic features, Omsk, p. 156.
2. Belskaya, L. V. et al (2008). Thermodynamic modeling of the formation of dental calculi, Herald of Omsk University, № 4, pp. 49–53.
3. Borowski, E. V. et al (1991). Oral Biology, Moscow: Medicine, p. 304.
4. Galiulina, M. V. (1988). Electrolyte components of mixed saliva in human physiology and pathology of the oral cavity, Moscow, p. 19.
5. Galiulina, M. V. et al (2000). Structural properties of mixed saliva, depending on the condition of the mouth, Omsk, pp. 44–48.
6. Golovanova, O. A. et al (2006). Spectral analysis of the quantitative essential trace elements in pathogenic bio minerals residents of the Omsk region, Applied Spectroscopy, T.73, № 6, pp. 792–796.
7. Leontiev, V. K. et al (1976). Biochemical Methods in Clinical and Experimental Dentistry, Omsk, pp. 32–33.
8. Leontiev, V. K. et al (1991). On the micellar condition saliva, Dentistry, № 5, pp. 17–20.

Ermakov[1] V., Danilova[1] V., Khushvakhtova[1] S., Degtyarev[1] A., Krechetova[1] E., Tyutikov[1] S., Buryak[2] A., Pytsky[2] I., Khabarov[2] B.

Differentiation of copper, molybdenum and tungsten in local biogeochemical cycles

[1]V.I. Vernadsky Institute of Geochemistry and Analytical Chemistry of RAS, Moscow

[2]A.N. Frumkin Institute of Physical Chemistry and Electrochemistry of RAS, Moscow *ermakov@geokhi.ru; akburyak@ipc.rssi.ru*

A comparative assessment of biogenic migration of Mo, Cu and W in different molybdenum-tungsten-copper deposits and background areas has carried out.

Key words: biogeochemistry, cycles, copper, molybdenum, tungsten, habitat, organisms

Reference: Akinfiev, N. N., A. V. Plyasunov (2012), On the problems of calculating the solubility of metal oxides in the vapor phase of water. *Vestnik ONZ RAN, 4 (doi:)*

Introduction

We have determined some trace elements content levels in soils, aquatic plants and/or animals (namely, in cattle blood & hair samples) in the conditions of some open cast deposits or background territories of the North Caucasus and Transbaikalia [*Ermakov, Soboleeva, 2008; Ermakov et al., 2011*]. The purpose of this study was to clarify the characteristics of accumulation of copper and molybdenum in animals on a background of different content of tungsten in the environment and feed and the possible inclusion of tungsten in the xanthine-oxidase of milk cows.

Methods

The field studies were conducted in summer, 2011 in the mining landscapes of tungsten & molybdenum deposits of Tyrnyauz, and in background areas of the North Caucasus through rocks, soil, waters, plants and/or animal sample selection. Determination of copper or molybdenum levels in most of the samples was measured by atomic absorption method using standard processes. The content of tungsten was determined by means of ICP-mass-spectrometry. The technique accuracy levels were checked using soil, plants or hair standard samples.

Results

It was established the enrichment the enrichment of soil-forming rocks by trace elements (Cu, Mo, W) in the Tyrnyauz area. The content of this elements here is higher the order, than in rocks of Chegem valley (background area). In water of Boksan-river and its inflows Zn concentration 1.5–7 times higher in comparison with Chegem-river waters. On some river-sites Mo, Pb, Ni and As concentrations are increased. It was discovered that soils of Baksan-river valley are significantly enriched with Mo и W (the enrichment coefficient (EC) 44–85 and 35–100, respectively), that is connected with displays of corresponding ore mineralization (Table 1).

Table 1. Parameters of biogenic migration of Mo and Cu in biogeochemical food chain

Object	Mo, mg/kg	Cu, mg/kg	EC	Kb
Anomal areas (Upper Mukulan, Tyrnyauz, Bilim)				
Water (8)	0.002–0.40	0.0027–0.076	5–400 (Mo) 2.2–2.7 (Cu)	
Soil, dump (8)	87–443	25.2–60.8	44–85 (Mo) 1.9–2.4 (Cu)	
Hay crop of plants (8)	7.2–64.5	3.0–10.6	14–20 (Mo)	0.08–0.29 (Mo) 0.12–0.17 (Cu)
Hair of cow (30)	1.33 ± 0.07	7.3 ± 0.2	13.3 (Mo)	
Blood of cow (20)	0.035 ± 0.07	0.61 ± 0.09	3.2 (Mo)	
Background areas (Baksan, Kizburun, Chegem, Aushiger)				
Water (9)	0.0004–0.001	0.001–0.0016		
Soil (12)	2.0–2.4	10.6–31.7		
Hay crop of plants (12)	0.5–3.2	1.8–12.4		0.25–1.33 (Mo) 0.16–0.39 (Cu)
Hair of cow (30)	0.1 ± 0.02	7.6 ± 0.3		
Blood of cow (20)	0.011 ± 0.03	1.03 ± 0.19		

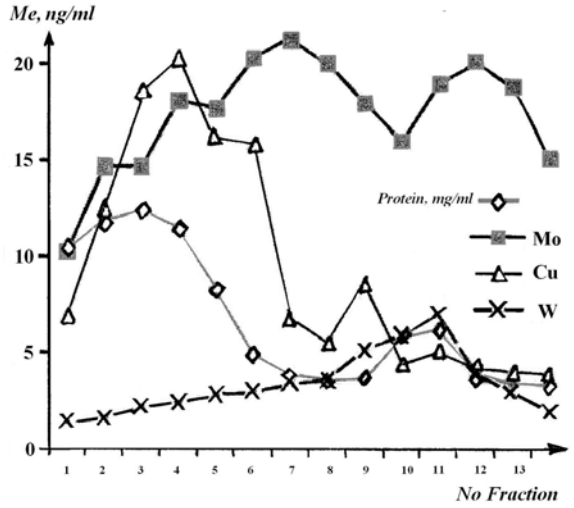

Fig. 1. Variation of concentration of metals, protein and activity of xanthine-oxidase in the fractions of prepared enzyme

EC in soils of the Chegem-river valley makes 1.2 for Mo and 7.7 for W. In soil of both regions of investigation the concentration of Zn is increased (EC 2.7 for Baksans valley and 2.2 – for Chegems valley). The quantity of Mo and Cu is some more higher in some plants. However, if the molybdenum content is increased in blood, milk and hair of cows, the level of copper significantly reduced compared with control animals areas.

Indicated metals were detected not only in cow milk, but in buttermilk too. При этом Their content is increased in buttermilk in 5–10 times as in mine areas, as in background sites herewith. So, the buttermilk of control site (Kudinovo) contained (in µg/l): Cu – 130, Mo – 93, W – 4, and in the product from cow milk from Tyrnyauza: Cu – 556, Mo – 684, W – 43 µg/l.

Taking into account known connection of molybdenum with the xanthine-oxidase, this enzyme was isolated from the buttermilk of animals from background territory (Kudinovo). It was discovered two fraction of this enzyme, predominantly containing Mo and Cu or Mo and W (Fig. 1).

Thus, in during biogeochemical investigations of W–Mo mine landscapes of the North Caucasus (Tyrnyauz) and background territories was discovered the accumulation of tungsten not only plant or soil microorganisms, but the including of this element in animal enzyme xanthine-oxidase. At increasing of molybdenum and tungsten level in the environment, the migration of last metal is enhancing very hard at mine areas.

Supported by grant of RFBR No. 12-05-00141-a.

References:

1. Ermakov, V., A. Soboleeva (2008). Migration of molybdenum under extremal geochemical conditions and its biological effects. *Trace elements in the environment - ecological and analytical problems,* Koszalin-Mielno (Poland), pp. 89–92.
2. Ermakov, V., L. Jovanovic, A. Degtyarev, V. Danilova, E. Krechetova, S. Tjutikov, S. Khushvakhtova (2011). The interrelation of copper and molybdenum in biogeochemical processes. *Ecologica,* vol.18, no. 63, pp. 363–367.

Experimental Geoecology

Artamonova S.Yu. Uranium oxides in technogenic aerosol of the area of Novosibirsk city

V. S. Sobolev Institute of Geology and Mineralogy of the Siberian Branch of RAS artam@igm.nsc.ru

In the article the first results of mineralogical and geochemical studying of the technogenic aerosols in area of Novosibirsk chemical concentrates plant (NCCP) are resulted. Content of uranium in technogenic aerosol are studied using ICP-MS, ICP-AES. Particles of uranium oxides are revealed in aerosol using electron microcsopy.

Key words: technogenic aerosol, uranium isotopes, uranium oxides, Novosibirsk, aerosol pollution, ecological risk

Reference: Artamonova, S. Yu. (2012), Uranium oxides in technogenic aerosol of the area of Novosibirsk city, *Vestnik ONZ RAS, 4, (doi:)*

In large cities of Siberia, there are many industrial enterprises being emission sources. Revealing local sources of pollution is of crucial importance for the improvement of urban and suburban ecology. In Siberia, snow is an ideal model object to study industrial emissions, because from early November to late March-early April, a steady snow cover contains solid aerosol particles as well as gaseous products adsorbed on solid phases. In winter, south and southwest winds prevail in the surface atmosphere layer of the Novosibirsk region, and in summer, the wind rose is more isometric [*Climat of Novosibirsk, 1979*]. At a height of 0.5 km in the boundary atmosphere layer, southwest and west winds are predominant. Therefore, aerosol emissions of the above industrial enterprises are spread mainly in the northeastern and northern directions.

NCCP – one of the greatest enterprises of Russian nuclear fuel cycles engaged in production of nuclear fuel for power and research reactors, lithium and its compounds which was founded in September, 25 1948.

Experimental part

Aerosol particles are accumulated in snow during winter. We test the snow samples. Volume of snow samples is about 70 l. To eliminate the pollution impact of highways, we took all samples at distances of more than 150 m from them. Intensity of aerosol pollution is estimated by ratio of aerosol to smelted smow volume (mg/l). Spread list of element in aerosol were detected in a wide range of concentrations by ICP MS on a Finnigan Mat mass spectrometer (Germany) with a U-5000AT+ aqueous-solution ultrasound atomizer. The detection limits of elements are listed in Table 1. ICP-AES on spectrometer IRIS Inc. is used additionally. Solid aerosol mass are dissolved by two alloying techniques with alkali KOH and $LiBO_2$. The relative standard deviation was up to 10%. Lower detecting limits were up 0.01 ppm. Ratio of isotopes $^{238}U/^{235}U$ is detected by ICP-MS, relative standard deviation was ≤ 2 %.

The integral elemental composition of solid aerosol particles was quantitatively determined by X-ray fluorescent analysis on synchrotron radiation (SR-XRFA) at the VEPP-3 Elemental-Analysis Station of the Institute of Nuclear Physics, Novosibirsk [*Artamonova, et al, 2007*]. This method permitted determination of 35 elements (Ti, V, Cr, Mn, Fe, Ni, Cu, Zn, Ga, Ge, As, Br, Mo, Ag, Cd, Sn, Sb, Te, Hg, Tl, Bi, Th, Pb, etc.) with detection limits of up to 0.1 ppm depending on the excitation energy of emission lines. The relative standard deviation was 10–15%. Soil standard SOIL-7 МАГАТЭ is used. X-ray diffraction analysis of aerosol particles was carried out on a DRON-3M powder diffractometer (CuK_α, U = 40 kV, I = 24 mA). This method permits a semiquantitative estimation of mass fractions of mineral phases. The morphology and chemical composition of aerosol particles were studied on an LEO 1430 VP scanning electron microscope equipped with an (EDS) OXFORD energy dispersion spectrometer. Scanning beam was ~0.5 μm in diameter, which permitted determination of the compositions of aerosol particles larger than 0.5–1 μm. Some spectra revealed intimate intergrowths of fine grains. The particles were examined in secondary and back-scattered electron images.

The method of reduction of brightness of a field of vision of an electronic microscope is applied to search iron oxides and other heavy particles (especially uranium oxides). The lower brightness is chosen, when iron oxides are seen as dark-grey particles, another more weight particles ≥ 56 atomic mass (for example, uranium oxides) are detected as brightly shone particles. More 5000 fields of vision of 212 μm X 159 μm in size are studied at an increase of 1500 times. There were about 300–500 aerosol particles with size > 0.5 μm are on one field of vision.

Results and discussion

In melted snow concentration of U is enough lower (mkg/l): mean 0.04, variation 0.02–0.06, Th concentration variation – 0.01–0.02. Соответственно Th/U=0.42.In solid aerosol particles content of Th is more in 2 times than content of U, and mean ratio Th/U = 2.12. On distance in 0.5 to 25 rm from NCCP radionuclide' content in aerosol and in melted snow is decreased in ~ 2 times. In aerosol mass mean U content is equal (ppm) 5.64, minimal U content – 4.50, maximal U content – 9.93. In aerosol mass mean Th content is equal (ppm) 11.74, minimal Th content – 8.80, maximal Th content – 15.49.

Natural U is the mixture of its isotopes: ^{238}U: ^{235}U: ^{234}U = 99.28 : 0.714 : 0.006, so natural ratio $^{238}U/^{235}U$= 139.05. For the first time it is revealed, that aerosol of NCCP area are enriched by ^{235}U, and in aerosol ratio $^{238}U/^{235}U$ is varied in range from 77.43 to 129.26. Mean $^{238}U/^{235}U$ in aerosol is equal 107.78.

Displacement of an isotope ratio $^{238}U/^{235}U$, high total contents U, Th in aerosols become geochemical indicators of NCCP emissions. No doubt, NCCP is source of significant technogenic aerosol pollution of surrounding.

Using scanning electronic microscope 10 aerosol particles of U oxides are found in aerosol mass. Range of U oxides particles size is from 2 to 18 $μм^2$. The particles are distinguished by their very high brightness under back-scattered electron images. The particles are represented as fragments of the wrong form which have stuck to alumino-silicate spheroids (fig.1). Stucking of weight U oxides fragment to hollow alumino-silicate microspheres get possibility for aerosol migration on a long distance.

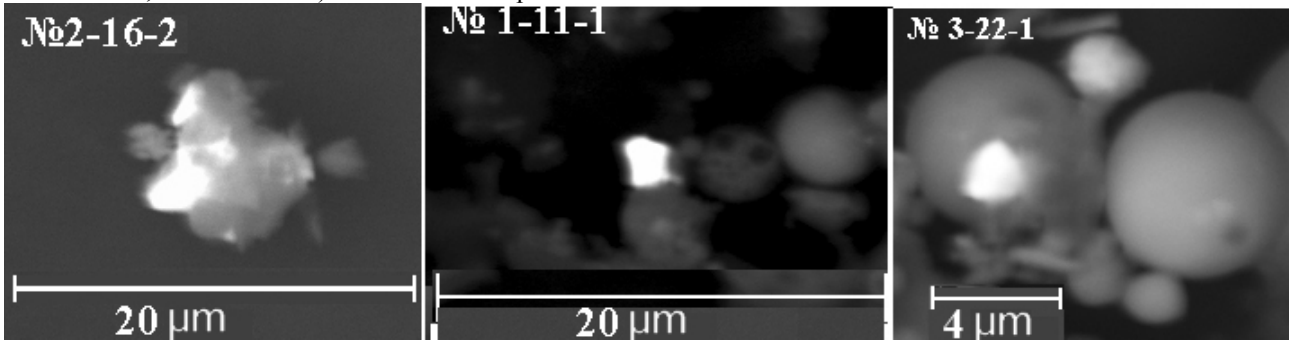

Fig. 1. Oxides of U, stucked to alumino-silicate particles and to hollow alumino-silicate microspheres

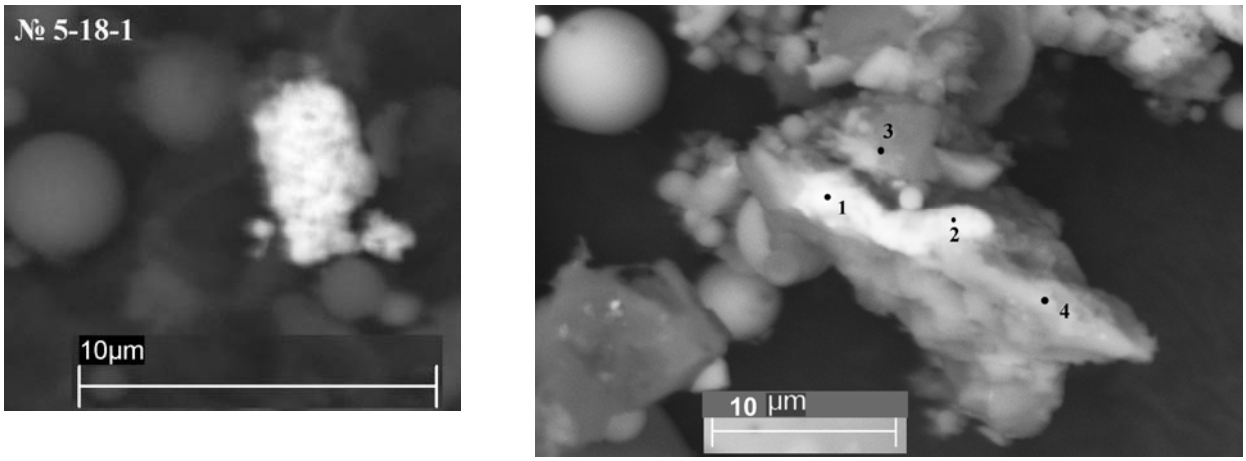

Fig. 2. Large slag aerosol particles with U (the element composition of right particle is shown in the table 2).

Table 1. Element composition of U oxides particles in technogenic aerosol of NCCP area

№ of the particle	Distance from NCCP, km	Size of the particle, μм^2	O , %	Fe, %	Cu, %	U, %
1—11-1	4.8	9	27.88	0	0	72.12
1—38-1	4.8	6	49.49	0.85	0	49.66
1—48-1	4.8	3	37.72	1.68	1.23	59.38
2—16-2	9.15	64	28.16	0.00	0.82	71.02
2-16-2a	9.15		52.81	3.19	0	44.00
2—18-1	9.15	6	34.39	0.98	0	64.63
2—32-1	9.15	8	23.90	0.99	0	75.11
3—22-1	9.15	3.9	65.18	0.98	0	33.83
4—14-1	17.5	12	26.00	1.54	1.09	71.37
4—22-2	17.5	2.25	37.18	2.11	0	60.71
5—9-1	22.8	3	25.89	1.34	0	72.77
5—18-1	22.8	18	21.20	0.00	0	78.80

Table 2. Element composition of the slag particle (fig. 2, on the right), %

№	O	Na	Mg	Al	Si	P	K	Ca	Ti	Fe	Y	Zr	U
1	48.31	0.77	0.55	3.71	13.02	1.74	0.37	0.85		17.83	3.77	6.8	2.28
2	48.92	1.49		4.28	14.9	1.95	2.04	1.06		6.96	6.05	9.87	2.47
3	56.76	1.37	1.98	8.98	22.07	1.09	1.76	0.58	0.37	5.04			
4	45.68	2.22		10.69	33.24		3.07			5.11			

Range of U content in U oxides particles is varied from 33.83 to 78.80 %. There are Fe – 3.19 %, Cu – 1.23 % in the particles (table.1). The one large particle of U oxides is found. Its size is 64 μм^2 in form of slag with a rough wavy surface (fig.2, at the left). The alunino–silicate slag particles riched Zr – 9.87 %, Y – 6.05 %, U – 2.47 % is found (fig 2, at the right, table 2).

Conclusions

The new date about NCCP emission is revealed. Technogenic aerosol of NCCP area are enriched by Th, U, especially by ^{235}U isotope, and mean ratio ^{238}U/^{235}U is 107.78. This technogenic U isotope ratio is smaller than natural ratio (natural ^{238}U/^{235}U is equal 139.05). For the first time aerosol particles of U oxides are found in aerosol mass of NCCP area.

The work was supported by RFBR grant № 09-05-00839 “Mineral-geochemical special features of the technogenic aerosols of Siberia”.

References:

1. Artamonova, S. Yu., A. S. Lapukhov, L. V. Miroshnichenko, L. I. Razvorotneva (2007). Mineral-Geochemical indicators of technogenic Sources of aerosol pollution, *Chemistry for Sustainable Development*, 15, p. 633–542.
2. *Climate of Novosibirsk*. Leningrad, Gidrometeoizdat, 221 pp (in russian).

Kotelnikov[1] A.R., Akhmedjanova[1] G.M., Suvorova[1] V. A., Martynov[2] K. V., Kovalsky[1] A. M. Matrix materials leaching stability

[1]Institute of Experimental Mineralogy RAS, Chernogolovka
kotelnik@iem.ac.ru
[2]A. N. Frumkin Institute of Physical Chemistry and Electrochemistry RAS, Moscow

The hydrolytic stability of some natural minerals (potential matrix materials for radionuclides immobilization) was carried out using

MCC-1 method. The high resistance of these minerals was demonstrated. The various synthetic mineral matrix materials were prepared using different methods (hot pressing, synthering, sorbtion and phase transformation, etc.). The examinations of the leaching stability of the synthetic mineral matrices were carried out by the method MCC-1 (at 90°C). The high stability of the synthetic materials was demonstated.

Key words: matrix materials, radionuclides, leaching stability

Ref: Kotelnikov, A. R. , G. M. Akhmedjanova1, V. A. Suvorova1, K. V. Martynov, A. M. Kovalsky (2012), Matrix materials leaching stability, *Vestn. Otd. nauk Zemle, 4*,

Suvorova V. A., Kovalskii A. M., Kotelnikov A. R. Method of synthesis of ceramic matrices for the radionuclides immobilization and its optimization

Institute of Experimental Mineralogy RASMoscow district, Chernogolovka *lera@iem.ac.ru*

Method of synthesis of matrix materials for radionuclides of rare-earth and alcaline-earth elements immobilization based on metasomatic replacement reactions using the scheme of «wet process» is presented in the work, the possibilities of its optimization are consider . This method allows spending process of radionuclides fixation on phosphate-containing mineral compositions at room temperature and atmospheric pressure under wet conditions. The results of synthesis of mineral matrices containing of binary (Sr, Na)- and (Ce, Na)- phosphates and also simple strontium and cerium orthophosphates are presented in the work.

Deficiency of solutions of Sr- or Ce- nitrates leads formation of mineral phases similar by composition to natural minerals olgite $NaSrPO_4$ or vitusite $Na_3Ce(PO_4)_2$. Simple orthophosphates of Sr and Ce were synthesized using of super quantities of nitrates solutions. For the further optimization of mineral matrice synthesis - decrease in temperature and increase of matrice density, the addition of Na- silicate in the form of liquid glass to solid mineral composition was used. As a result of experiments the polymineral ceramics consisting of feldspars, quartz, phosphates of strontium and cerium and small amount of Sr-containing glass have been received.

Key words: radionuclides immobilization, crystalline matrix materials, matrices synthesis.

Reference: Suvorova, V. A., A. M. Kovalskii, and A. R. Kotelnikov (2012), Method of synthesis of ceramic matrices for the radionuclides immobilization and its optimization, *Vestnik BES RAS, 4,*

The conception of phase and chemical correspondence in system matrix – solution – wallrock [*Kotelnikov et. al*., 1994] allow to optimize matrix materials for immobilization of the radionuclides of nuclear fuel cycle and suggest solid solutions of rock-forming and accessory minerals as stable matrices. Our experiments on investigation of leaching velocities of elements from natural minerals [*Kotelnikov et. al., 1999*] show that it is possible to recommend application of ceramic matrices based on accessory minerals of groups of phosphates, titanates and zirconates for fixing of rare earth and transuranium radionuclides. The techniques of hot pressing and sintering [*Ringwood et al.,* 1988*, Martynov et al.,* 1993] are usually used for synthesis of ceramic mineral matrices. However in this synthesis there is an unresolved problem of an initial material dispersion during mixing of matrice components. For its decision we used the scheme of «wet process» [*Kotelnikov et. al., 2005, Suvorova et. al., 2006, Suvorova et. al., 2012*].

Synthesis of phosphates was carried out using the metasomatic replacement reactions:

$$2Na_3PO_{4(s)} + 3Sr(NO_3)_{2(aq)} = Sr_3(PO_4)_{2(s)}\downarrow + 6NaNO_{3(aq)} \quad (1)$$

$$Na_3PO_{4(s)} + Ce(NO_3)_{3(aq)} = CePO_{4(s)}\downarrow + 3NaNO_{3(aq)} \quad (2)$$

The essence of these reactions is the replacement of the crystalline phase of sodium phosphate by slightly soluble strontium (cerium) phosphate and the removal of a soluble compound (sodium nitrate) into aqueous solution. In order to carry out the replacement reaction, strontium (cerium) nitrate solutions were filtered through columns from quartz glass filled with a model or natural granite and grains of crystalline sodium orthophosphate. The filtrate was collected in flasks and analyzed for strontium (cerium) and sodium. The mixtures of grains of natural feldspars (microcline, albite) and quartz (quartz sand in some experiments) were used as starting materials in the experiments on synthesis of granite matrix.

The filtrate was analyzed on containing of strontium (cerium) after the metasomatic replacement in columns. The matrices bringing from the columns were annealed at temperatures of 1100–1250°C during two hours. This resulted in the complete dehydration of aqueous phosphate and sintering of materials into massive aggregates. Products of experiments were investigated by the X-ray method; for an estimation of compositions of synthesized solid phases the microbeam method was applied.

Only up to 50 wt % of $Sr(NO_3)_2$ or $Ce(NO_3)_3$ water solutions were passed through the columns in the first experimental series. Then the columns were blocked up and the solution flow was completely passed off. After drying at 400°C and annealing at 1100°C, binary orthophosphates of Na and Sr or Na and Ce were diagnosed in columns.

Thus, the deficit of Sr- and Ce- nitrate solutions resulted in formation of mineral phases similar in composition to the natural minerals olgite $NaSrPO_4$ (Fig. 1) or vitusite $Na_3Ce[PO_4]_2$) (Fig. 2) in the column.

Simple strontium and cerium orthophosphates were synthesized with excess amount of nitrate solutions. In order to decrease the temperature of matrix sintering and increase its density the leucogranite of the Spokoininskoe deposit of Eastern Transbaikalia was used as a starting material instead of separate feldspar and quartz grains. Synthesis of mineral matrices was carried out by the method described above under the same optimal conditions. In these experiments, compulsory depression was created at the output of the column, which accelerated the solution flow and provided the completeness of its infiltration trough the leucogranite – Na phosphate mixture.

The experiments on metasomatic replacement with subsequent drying and annealing produced polymineral ceramic composites consisting of feldspar, quartz and strontium phosphate (Fig. 3) or cerium phosphate (Fig. 4). Phosphate of strontium is close by its structure to α-$Sr_3(PO_4)_2$ and cerium phosphate – to a mineral monazite-Ce ($CePO_4$).

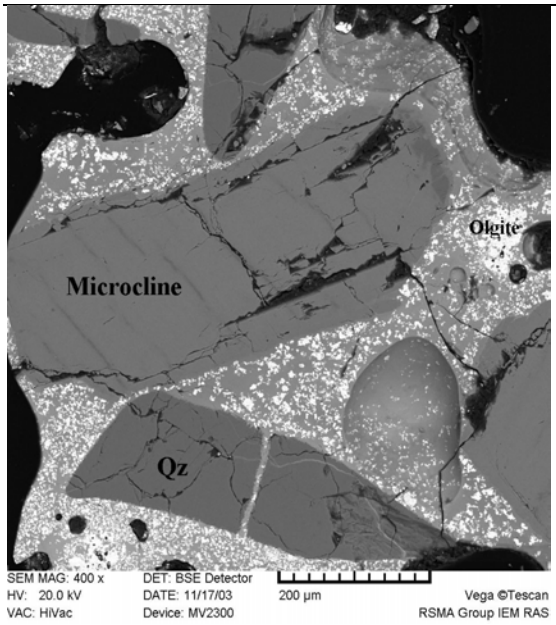

Fig. 1. Polymineral matrix on the basis of model granite for Sr immobilization in phosphate form. The small light grains on photo – phosphate Sr olgite ($NaSrPO_4$).

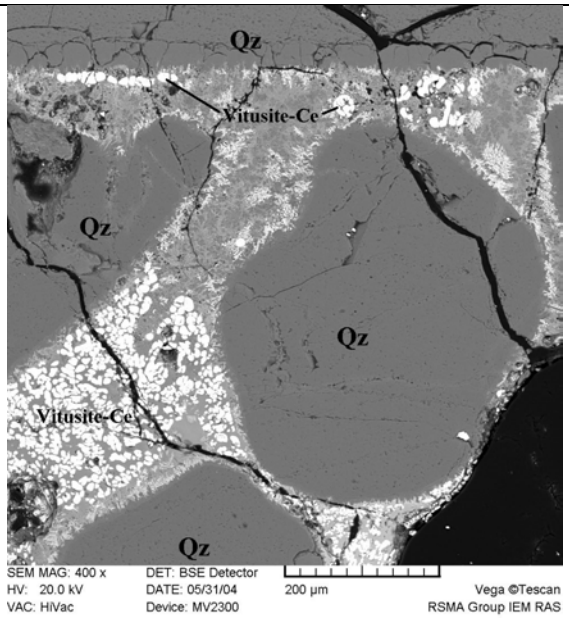

Fig. 2. Polymineral matrice on the basis of quartz sand for Ce immobilization in phosphate form. Light grains on photo – phosphate Ce vitusite ($Na_3Ce[PO_4]_2$).

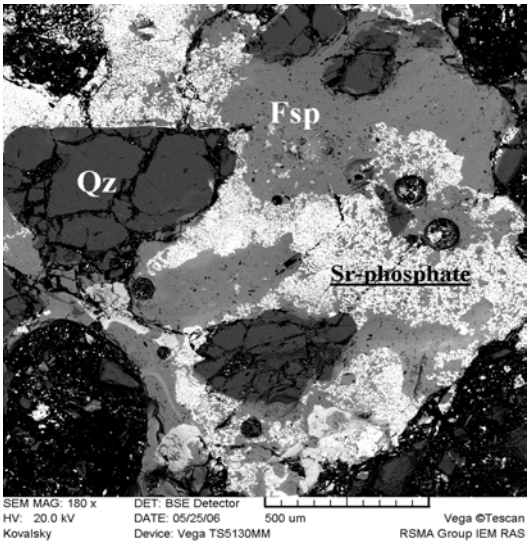

Fig. 3. Mineral matrice for Sr immobilization based on granite from the Spokoininskoe deposit containing strontium α-phosphate, $Sr_3(PO_4)_2$.

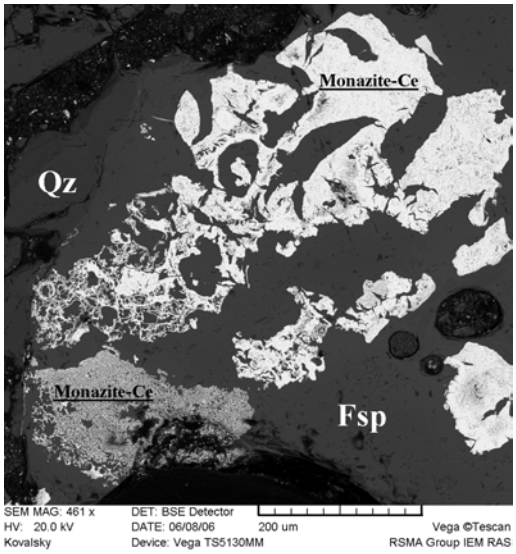

Fig. 4. Mineral matrice for Ce immobilization based on granite from the Spokoininskoe deposit containing Ce-monazite, $CePO_4$.

In details proven conditions of synthesis of mineral matrix materials allow to receive compact ceramics with the minimum surface for a leaching of components. Increase of density of the received crystal mineral composition for additional decrease of leaching velocities of matrix components may be reach by: 1) annealing of the received mineral composition in a column at the atmospheric pressure and temperature in an interval 900–1250ºC (depending on mineral composition of a silicate granite basis) or 2) hot pressing at the axial pressure of 700 kg/cm^2 and temperature in an interval 815–900ºC (depending on mineral composition of granite basis).

Method of synthesis of matrix material with addition of industrial liquid glass in composition was developed for optimization of process of ceramics synthesis (decrease in temperature of sintering and increase of matrix density). Na- silicate in the form of liquid glass with silica ratio equal 2 was added into a column after metasomatic replacement reaction. The increasing of speed of percolation of liquid glass through leicogranite grains was caused by assisted depression on an exit from a column. Further drying of ceramic composition without its unloading from a column was carried out at 110ºC within 24 hours. The cylindrical fragments of a column received as a result of hot pressing at 850ºC and axial pressure of 680 kg/sm^2. The products of experiments on synthesis of Sr- containing composition using such method consists of feldspar, quartz, strontium phosphate (white phases on fig. 5) and Sr-containing glass (small light-grey phases on fig. 5).

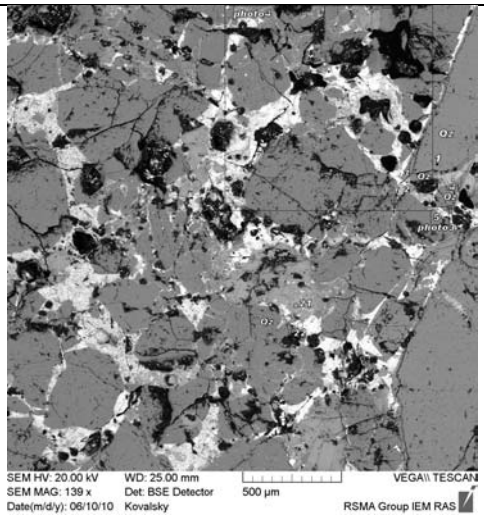

Fig. 5. Matrice for Sr immobilization in a mineral composition with addition of of liquid glass (Na- silicate).

In case of using of small-grained natural granite in experiences the eutectic melting on grain borders is reached at the minimum temperature. Such natural mineral composition can be recommended as an alumosilicate basis of a mineral matrice for immobilization of components of liquid high level waste of alcaline-earth and rare earth element groups in crystalline phosphate.

References:

1. Kotelnikov, A. R., G. M. Ahmedzhanova, V. A. Suvorova (1999), Minerals and their solid solutions - matrices for an immobilization of a radioactive waste, *Geochemistry international,* № 2, pp. 192–200.
2. Kotelnikov, A. R., A. M. Kovalskii, V. I. Tikhomirova et al. (2005), Mineral matrices for immobilization of radioactive waste elements: new possibilities of «wet process», *Materials of 15th Russian conference on experimental mineralogy*, Syktyvkar, Inst. Geol. Komi SC UrO RAS, pp. 468–470 (in Russian).
3. Kotelnikov, A. R., V. N. Zyryanov, M. B. Epelbaum (1994), Concept of phase and chemical correspondence during disposal of high level waste in the crustal rocks, *In book: Geochemical problems of the immobilization of radioactive waste*, Miass, pp. 83–103 (in Russian).
4. Martynov, K. V., K. I. Gushchin, G. M. Akhmedzhanova et al. (1993), Synthesis and study of properties of ceramic matrices on the base of minerals of complex oxide group containing of RAW emulator, *Materials of 4th annual scientific–technical conference of nuclear society on nuclear energy and safety NE-93*, Nizhnii Novgorod, p. 2, pp. 968–969 (in Russian).
5. Ringwood, A. E., S. E. Kesson, K. D. Reeve et al. (1988), SYNROC, Radioactive waste forms for the future, *Ed. by W. Lutze and R. C. Ewing,* Elsevier, New York, pp. 233–334.
6. Suvorova, V. A., A. M. Kovalskii, A. R. Kotelnikov, G. M. Akhmedzhanova (2012), «Method of alcaline-earth and rare-earth elements radionuclides immobilization in the mineral matrice», *Patent for an invention №2444800,* The priority of invention from 15.12.2010*,* Registered in the state register of inventions RF 10.03.2012 (in Russian).
7. Suvorova, V. A., V. I. Tikhomirova, A. M.Kovalskii, Akhmedzhanova G. M., Kotelnikov A. R. (2006), Synthesis of matrix materials for an immobilization of radionuclides on the method of «wet process», *Materials of annual a seminar on experimental mineralogy, petrology and geochemistry ESEMPG-2006,* Moscow, GEOCHI RAS, p. 70 (in Russian).

Suvorova V.A., Ahmedzhanova G.M. The mechanism of transformation of hydrophosphates (Na,Ce) and (Na,Sr) in reactions of metasomatic replacement under the scheme of "wet process» immobilization radionuclides

Institute of experimental mineralogy RAS, Chernogolovka.
lera@iem.ac.ru

Results of research of interaction are given in system: phosphate - containing mineral composition – Sr or Ce nitrate – Sr or Ce phosphate. Methods element, X-ray and AAS analyses investigated conditions at which practically all phosphate of sodium entering into initial mineral composition, it is possible to replace with insoluble phosphates of the corresponding radionuclides (Sr or Ce). In such a way received phosphates are those phases in the synthesized mineral matrixes which hold radionuclides.

Keywords: radioactive waste, mineral matrixes, speeds of processes, immobilization of radionuclides of Sr and Ce

Reference: Suvorova, V. A., G. M. Akhmedzhanova (2012), Mechanism of transformation of hydrophosphates (Na, Ce) and (Na, Sr) in reactions of metasomatic replacement according to the scheme of «wet process» immobilization of radionuclides, *Vestnik ONZ RAS, 4,*

Ceramic materials based on titanates, zirconates, and complex phosphates are produced for the immobilization of rare-earth and actinide radionuclides by the methods of hot pressing and sintering [*Ringwood et al., 1988, Martynov et al., 1993*]. In work [*Suvorova et al., 2009*] the method of matrix material synthesis on the basis of metasomatic replacement reactions according to the scheme of «wet process» [*Kotelnikov et al., 2005*] is described. Process of replacement can be carried out at room temperature and atmospheric pressure. Strontium and cerium phosphates were synthesized using the following reactions:

$$2Na_3PO_{4(s)} + 3Sr(NO_3)_{2(aq)} = Sr_3(PO_4)_{2(s)}\downarrow + 6NaNO_{3(aq)} \quad (1)$$
$$Na_3PO_{4(s)} + Ce(NO_3)_{3(aq)} = CePO_{4(s)}\downarrow + 3NaNO_{3(aq)} \quad (2)$$

The essence of these reactions is the replacement of the crystalline phase of sodium phosphate by slightly soluble strontium (cerium) phosphate and the removal of a soluble compound (sodium nitrate) into aqueous solution. In work interaction processes phosphate - containing mineral compositions with Sr or Ce nitrates, and also pure Na phosphate with the same nitrates are investigated.

The essence of these reactions is the replacement of the crystalline phase of sodium phosphate by slightly soluble strontium (cerium) phosphate and the removal of a soluble compound (sodium nitrate) into aqueous solution.

In order to carry out the replacement reaction, strontium (cerium) nitrate solutions were filtered through columns filled with a model or natural granite and grains of crystalline sodium orthophosphate.

Behavior of Sr and Ce at interaction with calcinated Na_3PO_4

Starting materials. Anhydrous sodium orthophosphate was obtained by drying and annealing at 1100°C of $Na_3PO_4 \times 12H_2O$ reagent was attained, which resulted in the sintering of individual crystallites into polycrystalline aggregates. In columns with fraction of a starting mix 0.40÷0.63 mm speed of solution infiltration provided course of exchange reactions in phosphates therefore this

fraction was chosen for carrying out reactions of metasomatic replacement.

In order to carry out the replacement reaction in a initial series of experiences solutions of nitrates of strontium were filtered through the columns filled with a model granite and grains of crystal orthophosphate of sodium (25 mas.% from mix weight). To receiving a model granite applied mixes of grains albite (90 mas.%) or a microwedge (85 mas.%) and quartz (10 ÷ 15 mas.%).

In preliminary experiences through columns with mixes it is flowed within 5 days by portions of 6.86 ml 1M $Sr(NO_3)_2$ solution. After the first portion (1.5 ml of solution) replacement was sharply broken since the stopper from the formed jellylike hydrophosphate of strontium – $SrH(PO_4)$ - didn't pass the next portion of solution. In every portion of the proceed filtrate defined the composition of Sr. In a filtrate from a column with Mic of strontium isn't present, it replaced all in $Sr_3(PO_4)_2$ and $NaSrPO_4$ which have settled in a column. In a column with Ab there was an insignificant quantity of Sr.

For comparison in static conditions (without a channel of new portions of solution) experiments on interaction of phosphate of sodium with the distilled water, with 1M $Sr(NO_3)_2$ solution and with Mic+Qz mix + Na_3PO_4 + 1M $Sr(NO_3)_2$ were made. The composition of Sr and Na defined, separating a solution share. Results of these experiences are presented in table 1.

Table 1. Change of composition of Sr and Na during exchange reactions with phosphate Na_3PO_4.

Composition	Duration of contact	[Na], mg/ml	[Sr], mg/ml
Mic+Qz + Na_3PO_4 + $Sr(NO_3)_2$	5 days, column N 4	1.06	0.0
Ab+Qz + Na_3PO_4 + $Sr(NO_3)_2$	5 days, column N 2	145.0	0.012
Na_3PO_4 + 6.86 ml H_2O	2 hour, static	315.0	-
Na_3PO_4 + 6.86 ml $Sr(NO_3)_2$	2 hour, static	21.6	51.0
Mic+Qz + Na_3PO_4 + $Sr(NO_3)_2$	2 hour, static	46.0	23.0

In the composition of the solid phase which has remained in reactionary capacity, except Mic+Qz, there is $Sr_3(PO_4)_2$ and $NaSrPO_4$. Experiments on interaction of sodium phosphate mixed with Mic+Qz or Ab+Qz in static conditions were carried out also with 1M $Ce(NO_3)_3$ solution. In the composition of the solid phase in both experiences, except Mic+Qz or Ab+Qz, there is $CePO_4$ and $Na_3Ce(PO_4)_2$.

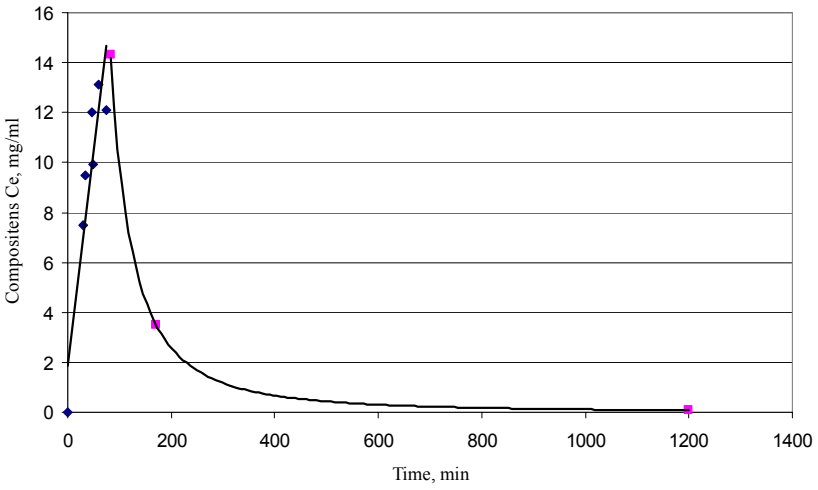

Fig. 1. Kinetics of change of he Ce contents in a product of reaction of a granite - phosphatic mix with 0.1M $Ce(NO_3)_3$ solution.

The interaction kinetics in a column of $Ce(NO_3)_3$ solution of the various concentration with various model granite mixes is investigated, is the most detailed - filtration kinetics 0.1M $Ce(NO_3)_3$ solution through a column filled with a granite-phosphatic mix. Composition of Ce defined in portions of the replaced filtrate. The salt which slipped into a filtrate - rabdofonite CePO4×nH2O, where n = 0,5-1,5. Results of this experience are presented on fig. 1.

As appears from fig. 1 in process of intake of solution the maintenance of Ce grows as solution is spent for Na phosphate moistening. that leads to its hydrolysis. Emergence of NaOH leads to formation of a hydroxide of Ce – Ce $(OH)_3$. Gradually hydrolysis chokes with the additives of Ce $(NO_3)_3$ solution leading to growth of concentration of Ce. Eventually, accumulation of badly soluble hydroxide leads to obstruction of a column and reduction of filtrate exit.

In 2 hours in plum CePO4 salt loss - a product of interaction of the arrived Ce (NO3) 3 solution with neogenic Na hydrophosphate was observed. Reduction of concentration of Ce began. The filtrate went very slowly. The mechanism of this interaction can be described the following scheme:

$$Na_3PO_4 + H_2O = Na_2HPO_4 + NaOH \quad (3)$$

$$Ce(NO_3)_3 + 3\,NaOH = Ce(OH)_3 + 3\,NaNO_3 \quad (4)$$

$$Na_2HPO_4 + Ce(NO_3)_3 = \underline{CePO_4}\downarrow + 2\,NaNO_3 + HNO_3, \quad (5)$$

$$Na_2HPO_4 + HNO_3 = NaNO_3 + NaH_2PO_4 \quad (6)$$

This mechanism proves to be true also other columnar experiences with Sr and Ce nitrates. Results of these experiences are presented in table 2 and in drawing 2.

A) Table 2. Change of Sr and Na contens during experience with 1M Sr (NO3) 2 solution

Duration of interaction, min	37	42	47	67	80	122
Content Sr, mg/ml	32	27.3	25.5	30	34	8.5
Content Na, mg/ml	3	-	-	-	-	22.5

B)

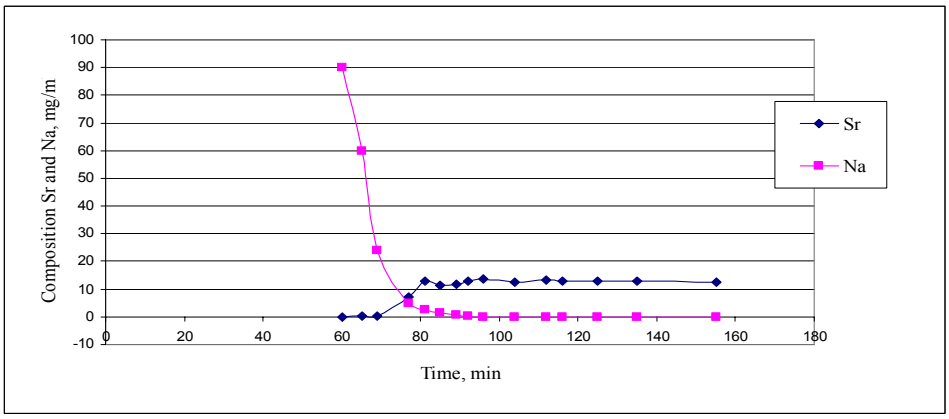

Fig. 2. Kinetics of change of Sr and Na contents in a reaction product phosphate - containing composition with 0.2M $Sr(NO_3)_2$ solution

C) Similar experiences with 1M Ce $(NO_3)_3$ solution too show a small amount of sodium in a filtrate (17 mg/ml) - solution of nitrate is spent for Na phosphate hydrolysis.

So, in all columnar experiences similar nature of interaction – formation of the connection interfering course of settlement amount of nitrate solutions that leads to the premature termination of reagents interaction is observed. To define optimum parameters of «wet process» immobilization of radionuclides, a series of experiments on interaction of nitrates of these nuclides with a pure reactant of $Na_3PO_4x12H_2O$ was carried out.

Behavior of Ce and Sr at interaction with Na_3PO_4 x12H_2O

1. Static conditions

Ce: In each of 6 capacities it is placed on 250 mg of $Na_3PO_4x12H_2O$ and it is flowed on 6,6 ml 0.2M $Ce(NO_3)_3$ solution. By the expiration of chosen time determined the conten of Ce in solution from the next capacity. It practically didn't change, as it is presented in table 3.

Sr: The similar technique was used in experiences with 0.2M $Sr(NO_3)_2$ solution. Results are presented on fig. 3.

Table 3. Change of Ce content in reaction products with 0.2M $Ce(NO_3)_3$ solution.

Duration of interaction, min	50	130	220	1200	2460	3880
[Ce], mg/ml	20.3	20.5	21.5	22.7	18.9	18.2

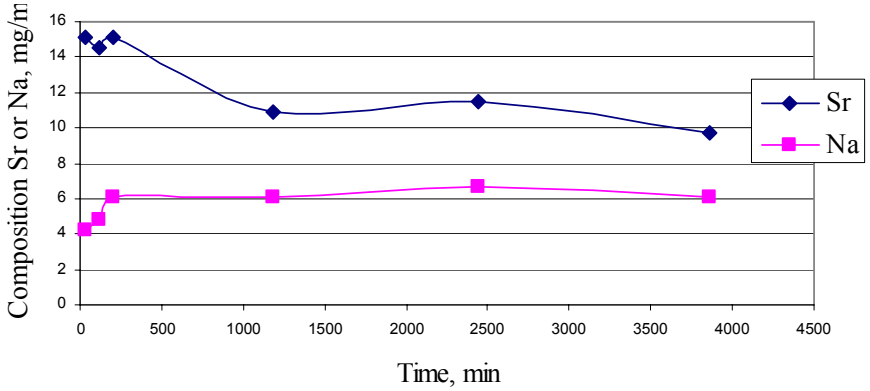

Fig. 3. Dependence on duration of interaction with 0.2M $Sr(NO_3)_2$ solution of Sr and Na contents in a reaction product with Na_3PO_4 x12H_2O

Apparently from drawing 3, Na_3PO_4 was hydrolyzed with formation of the soluble forms which have defined increase of sodium concentration within the first 20 hours. For this short period the content of strontium in solution only it was designated, and then began to fall since there passed reaction of replacement of $Sr(NO_3)_2$ to settling $Sr_3(PO_4)_2$. Concentration of both elements, as well as cerium (see tab. 3), remain after about 20 hours constants, despite long endurance.

2. Kinetic conditions

Ce: Through a column in which 1 g of Na_3PO_4 x 12H_2O is placed, it is flowed by portions of 18 ml 0.2M $Ce(NO_3)_3$ solution. Results of this experience are presented in table 4.

Sr: The similar technique was used in experiences with 0.2M $Sr(NO_3)_2$ solution. Results are presented on fig. 4.

Table 4. Change of Ce content in a product of reaction of Na_3PO_4 x12H_2O with 0.2M $Ce(NO_3)_3$ solution

Duration of interaction, min	15	960	970	1200	1220	1305
[Ce], mg/ml	0.034	0.440	0.466	0.510	-	0.910

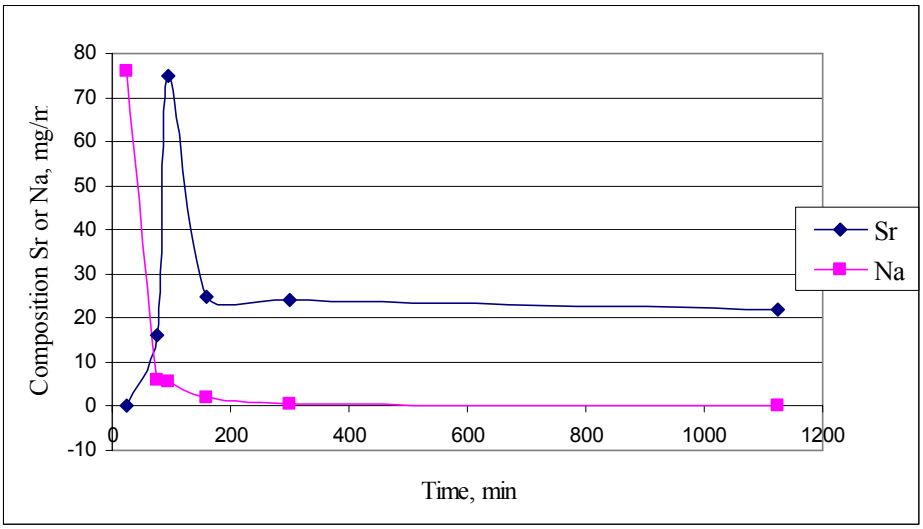

Fig. 4. Kinetics of change of Sr and Na contents in a product of reaction of Na_3PO_4 x $12H_2O$ with 0.2M $Sr(NO_3)_2$ solution

In these experiences – with participation few the concentrated solutions, as well as in all columnar experiences, it is possible to observe initial sharp growth of concentration of cerium and strontium though at cerium it comes later. Then concentration of both elements fall since there passes reaction of replacement of $Sr(NO_3)_2$ to settling $Sr_3(PO_4)_{2(s)}$ on reaction (1) or $Ce(NO_3)_3$ on settling $CePO_{4(s)}$ on reaction (2). Having sharply fallen, they remain constants, despite long endurance, i.e. further interaction doesn't occur owing to formation of the jellylike hydrophosphates interfering contact of reactants. Judging by amount of sodium in a filtrate, its replacement occurs actively, and it is spent up to the end.

References:

1. Ringwood, A. E., S. E. Kesson, K. D. Reeve, D. M. Levins, E. J. Ramm (1988). SYNROC, *Radioactive waste forms for the future*, Eds.: W.Lutze and R.C.Ewing, Elsevier Sci. Publ., Ch. 4. 324 p.
2. Martynov, K. V., K. I. Gushchin, G. M. Akhmedzhanova, O. A. Volegova (1993). Synthesis and Study of the Properties of Ceramic Matrix Made up of Minerals of Compound Oxide Groups Simulating RAW, *4th Annual Scientific–Technica Conference of Nuclear Society on Nuclear Energy and Safety NE-93*, Nizhnii Novgorod, Part 2, pp. 968–969 (in Russian).
3. Suvorova, V. A., A. M. Kovalskii, A. R. Kotelnikov (2009). Synthesis phosphate - containing matrixes a method of metasomatic replacement reactions, *Geochemistry*, No. 11, P. 1216-1222.
4. Kotelnikov, A. R., A. M. Kovalskii, V. I. Tikhomirova, et al. (2005). Mineral Matrix for the Immobilization of Elements from Radioactive Wastes: New Possibilities of a «Wet process», *Proceed. of 15th Russian Confer. on Exper. Mineralogy*, Inst. Geol. Komi NTs UrO RAN, Syktyvkar, 2005, pp. 468–470 (in Russian).

Tyutyunnik [1]O. A., Levinsky[2] V. V., Kundryakov [2]V. V., Kuzovlev[2] V.V., Getsyna[1] M.L. Toropchenova[1] E.S. Complex research of water and bottom sediments of the Tmaka river in Tver city

[1] V. I. Vernadsky Institute of Geochemistry and Analytical Chemistry RAS, Moscow NMlab@geokhi.ru, v-levinsky@mail.ru
[2]Tver State Technical University

As a result of comprehensive research of water and bottom sediments of the Tmaka River the estimation of the water quality in terms of SCWPI (specific combinatorial water pollution index) and the criteria of toxicity for aquatic organisms are given. Pollutants priority for the Tmaka River (Ba, Cd, Cr, Cu, Mn, P, Pb, Sr, Zn, Hg, as well as oil products), are identified. Special attention in the monitoring of river and wastewater of the city should be given to the elements mentioned.

Key words: ecology, pollution of water and bottom sediments, biogenic matter, organic matter, anthropogenic pollution

Ref: Tyutyunnik, O. A., V. V. Levinsky, V. V. Kundryakov, V. V. Kuzovlev, M. L. Getsyna, E. S. Toropchenova (2012), Complex research of water and bottom sediments of the Tmaka river in Tver city, *Vestnik ONZ RAS, 4,*

The complex investigation on the assessment of water quality and the identification of the most polluted sites of the Tmaka River has been conducted. Recommendations have been given on the development of the system of ecological monitoring of the river.

The Tmaka is the right tributary of the Volga. The length of the Tmaka is 73 km, the catchment area is 582 km^2. The main source of water feeding of the river is snow (more than 50 % of annual volume). Rain waters give 15–20 % and ground waters give 30–35 % of annual volume.

Throughout all its length the river suffers the anthropogenous influence. In the upper and medium stream the river accepts the runoff from drying peatlands and agricultural grounds. In the lower stream (including Tver) the river is used for recreation and as the receiver of household, storm water and production sewage. The last 11 km of the lower stream of the river within the city have been studied in this work.

Four water sampling points on the river were chosen which characterize the different level of anthropogenous pressing: No.1–11 km upstream the mouth of the river

(background point), No.2–7 km upstream the mouth (residential area), No.3–4 km upstream the mouth (industrial area), No.4–0.3 km upstream the mouth (before the flowing into the Volga).

The samples of water were taken during the main hydrological phases in the period from May 2010 till June 2011. The following indices were determined in water:

1) Hydrolodical (water level);
2) Physical (water temperature, conductivity, color, turbidity, smell);
3) Dissolved oxygen;
4) pH and Eh;
5) The main ions (HCO_3^-, SO_4^{2-}, Cl^-, Ca^{2+}, Mg^{2+}, Na^+, K^+);
6) Biogenic components (NH_4^{2+}, NO_2^-, NO_3^-, Phosphates, Total iron, Si);
7) Permanganate oxidizability (PO);
8) Oil products (OP) and heavy metals (Zn^{2+}, Cd^{2+}, Pb^{2+}, Cu^{2+}).

Temperature, pH, Eh, dissolved oxygen and conductivity were measured *in situ*. Zinc, cadmium, lead and copper were measured with a method of inversion voltammetry on a mercury film electrode [*ФР.1.31.2004.00987 (2009)*].

Statistical parameters (maximal, minimal and medium concentrations, standard deviation) of the examined indices are given in table 1. Complex assessment of water quality with using of combinatory indices of pollution [*РД 52.24.643-2002 (2002)*] are shown in table 2.

During low water on March 23, 2011 the samples of water and bottom sediments were taken for the detailed microelement analysis. The maximum concentrations of all the tested elements were found in the mouth of the Tmaka (table 3).

Besides the chemical studies the biological testing was carried out of the samples of water and water extracts of bottom sediments using *Daphnia magna Straus* and *Chlorella Vulgaris Beijera* [*ФР.1.39.2007.03222 (2007), ПНДФ Т 14.1:2:3:4.10-04*]. In all the samples the intensive development of alga was observed. There is a correlation between toxic frequency rate of diluting of water and concentration of ammonium in water. In the bottom sediments' extracts the increasing of toxicity was recorded downstream the river from "slightly toxic" to the "hyper toxic".

By the results of biotesting with using *Daphnia* no toxic influence was revealed in spite of the high content of many pollutants, in particular, metals: iron, manganese, molybdenum and mercury. The results allow assuming that the complex formation occurs of these metals with some natural ligands and, as a result, their toxicity is decreasing [*Edigarova I.A. (1989)*].

It was shown that most serious impacts on the river Tmaka within the city of Tver are the following:

1. Communal waste water discharge in Nikolsky settlement causes pollution of the river by biogenic elements, detergents and pathogenic microorganisms;
2. Disposal of oil reservoirs near Nikolsky within water protection zone of the river creates the risk of pollution of ground waters and storm drain by oil products;
3. Disposal of ash residues from the heating station on the right bank of the river can be the source of polluting substances going to the river with ground waters;
4. Private housing estate on the right bank can be the source of sewage from the houses and grounds.
5. Sand extraction near Stroiteley St. causes the destruction of the right bank and dumping of the wastes.
6. Industrial waters going from the heating station, the Proletarka factory, the worsted plant and the Rozhdestvenskaya textile mill lead the increasing of water temperature in Tmaka;
7. Automobile bridges crossing the river can be the source of oil and salt pollution;
8. There are many damps and fallen trees on banks and bed of the river.
9.

The water pollution, the declining of self-cleaning processes, the soiling of riverbed and the eutrophication of the river are the results of intensive anthropogenous impact on the Tmaka.

In the lower course of the river the accumulation of Ba, Cd, Cr, Cu, Mn, P, Pb, Sr, Zn, Hg and oil products is under way. These substances should be entered in the list of specific substances for the ecological monitoring of the Tmaka and the monitoring of the industrial sewages.

Table 1. Values of hydrochemical indices in water samples of the river Tmaka

Sample point No	Index	Color	pH	h	NH_4^{2+}	NO_2^-	NO_3^-	PO_4^{2-}	Fe^{3+}	Si	PO*	HCO_3^-	Ca^{2+}	Mg^{2+}	Na^+	SO_4^{2-}	Mn^{2+}	Cl^-	K^+	O_2	OP**	Zn^{2+}	Cd^{2+}	Pb^{2+}	Cu^{2+}
1	Max C	166	8.2	600	**1.84**	**0.090**	13.1	**0.27**	**1.97**	6.04	48	319	85	21	9.6	98	0.90	31	2.0	14	0.032	0.0006	0.0036	0.0055	<0.0006
	Min C	40	6.9	199	**0.58**	0.001	0.65	<0.01	0.18	0.94	1.6	94	36	0	3.1	0	<0.01	3.4	0.7	2.8	0.007	<0.0005	<0.0002	<0.0002	<0.0006
	$\overline{C}$	92	7.5	312	**0.98**	0.034	3.29	0.07	**0.75**	3.16	22	219	63	11	5.1	25	**0.25**	12	1.4	8.1	0.018	0.0002	0.0010	0.0014	<0.0006
	σ	42	0.4	138	0.40	0.030	3.65	0.11	0.64	2.10	14	82	18	6.1	2.4	29	0.39	8.6	0.6	3.0	0.009	0.0002	0.0011	0.0017	0
2	Max C	165	7.9	476	**1.84**	**0.097**	12.3	**0.29**	**1.69**	5.92	45	299	81	21	8.9	96	**0.87**	25	2.2	10	0.023	0.0014	0.0031	0.0052	<0.0006
	Min C	41	6.8	208	0.44	0.000	1.30	<0.01	0.12	0.86	3.2	97	38	0	3.1	0	<0.01	3.4	0.7	2.2	0.006	<0.0005	<0.0002	<0.0002	<0.0006
	$\overline{C}$	91	7.4	273	**0.91**	0.041	3.65	0.08	**0.64**	2.96	20	220	62	12	6.1	31	**0.25**	13	1.4	7.3	0.015	0.0005	0.0008	0.0019	<0.0006
	σ	42	0.4	72	0.44	0.037	3.25	0.12	0.54	2.05	13	79	17	8.0	2.6	34	0.40	7.0	0.6	2.5	0.007	0.0004	0.0009	0.0020	0
3	Max C	157	7.9	650	**1.88**	**0.115**	12.3	**0.27**	**1.73**	5.80	35	265	75	17	9.6	78	**0.44**	22	2.7	10	0.021	0.0009	0.0020	**0.0064**	0.0006
	Min C	39	6.5	200	0.44	0.000	1.01	0.00	0.10	0.86	3.2	97	40	0	2.6	0	0.02	3.8	0.7	5.1	0.013	<0.0005	0.0002	0.0007	<0.0006
	$\overline{C}$	86	7.4	373	**1.01**	0.045	3.50	0.07	**0.64**	2.86	16	201	56	9.8	5.8	25	**0.15**	12	1.4	8.1	0.017	0.0005	0.0008	0.0031	<0.0006
	σ	41	0.4	171	0.43	0.043	3.38	0.11	0.63	1.85	13	62	11	5.8	2.7	24	0.20	5.9	0.6	1.9	0.003	0.0004	0.0005	0.0020	0.0002
4	Max C	154	8.3	600	**1.90**	**0.132**	12.3	**0.41**	**1.25**	5.88	42	274	74	16	23	84	**0.65**	26	6.3	10	**0.075**	0.0009	0.0030	**0.0065**	**0.0017**
	Min C	31	6.9	195	0.36	0.003	0.50	0.00	0.06	0.28	4.8	97	36	0	2.4	0	<0.01	4.4	0.7	6.8	0.005	<0.0005	0.0005	0.0033	<0.0006
	$\overline{C}$	79	7.5	340	**0.94**	0.051	3.80	0.08	**0.53**	2.95	17	204	56	9.5	8.4	21	**0.17**	14	2.2	8.4	0.031	0.0006	0.0018	0.0047	<0.0006
	σ	40	0.4	144	0.51	0.047	3.40	0.15	0.44	2.13	11	63	13	5.4	7.1	26	0.26	7.5	1.8	1.0	0.022	0.0002	0.0010	0.0012	0.0007

PO* - Permanganate oxidizability, OP** - Oil products Concentrations which exceed the admissible concentration limit are allocated with a bold print

Table 2. Combinatory indices of pollution of water in four points of the River Tmaka in Tver

Point No.	CWPI*	SCWPI**	Quality class	Priority pollutants (in descending order)
	37.46	2.34	Polluted (3 a)	Mn, Fe,NH_4^+, PO_4^{3-}, deficiency in O_2
	39.02	2.44	Very polluted (3 b)	Mn, Fe, NH_4^+, PO_4^{3-}, deficiency in O_2, NO_2^-
	40.69	2.54	Very polluted (3 b)	Mn, Fe, NH_4^+, NO_2^-, deficiency in O_2, PO_4^{3-}, Pb
	47.21	2.95	Very polluted (3 b)	Mn, Fe, NH_4^+, PO_4^{3-}, NO_2^-, Cu, Pb

* Combinatory water pollution index
** Specific water pollution index [*РД 52.24.643-2002 (2002)*].

Table 3. Concentrations of microelements in samples of water and bottom sediments of the Tmaka

Bottom Sediments	**As**	**Ba**	**Be**	**Cd**	**Co**	**Cr**	**Cu**	**Li**	**Mn**	**Mo**	**Ni**	**P**	**Pb**	**S**	**Sr**	**Ti**	**V**	**Zn**	**Hg**
Sample point No 1	0.40	43.9	0.17	22	1.8	3.67	6.01	4.4	198	0.3	4.5	542	0.9	2299	8.4	209	7.06	9.05	<20
Sample point No 2	0.30	39.6	0.13	22	1.5	2.93	6.76	3.5	152	0.4	3.8	401	1.0	2279	10.7	168	5.52	9.68	<20
Sample point No 4	0.75	99.9	0.25	90	3.04	12.1	54.2	7.19	483	0.29	7.9	1500	9.09	4009	24.2	258	10.1	46.4	80,5
Water	**Al**	**As**	**Ba**	**Ca**	**Cd**	**Co**	**Cr**	**Cu**	**Fe**	**Li**	**Mg**	**Mn**	**Mo**	**Na**	**Ni**	**Si**	**Sr**	**Zn**	**Hg**
Sample point No 1	0.016	<0.0001	0.049	52.9	<0.00001	<0.002	<0.002	<0.001	**1.95**	0.003	14.4	**0.81**	**0.009**	6.81	<0.002	5.04	0.14	0.006	<10
Sample point No 2	0.011	<0.0001	0.046	53.9	<0.00001	<0.002	<0.002	<0.001	**1.01**	0.003	14.9	**0.81**	**0.007**	8.27	<0.002	5.10	0.15	0.006	<10
Sample point No 4	0.018	<0.0001	0.044	53.8	<0.00001	<0.002	<0.002	<0.001	**1.77**	0.003	14.4	**0.71**	**0.008**	9.05	<0.002	4.90	0.18	0.003	**11**

Concentrations which exceed the admissible concentration limit are allocated with a bold print

References :

1. Edigarova, I. A., V. N. Krasyukov, I. A. Lapin, A. M. Nikanorov (1989). Complex-forming ability of the dissolved organic substance of the natural waters, *Water Resources*, No. 4, pp. 122–129.
2. ПНДФ Т 14.1:2:3:4.10-04. A method of determination of toxicity of samples of superficial fresh, soil, drinking, sewage, water extracts from soils, sewage sediments and wastes on change of optical density of culture of *Chlorella vulgaris Beijer*.
3. РД 52.24.643-2002 (2002). *Methodical instructions. A method of a complex assessment of degree of contamination of a surface water on hydrochemical indicators.* Moscow: Federal Hydrometereology and Environmental Monitoring Service.
4. ФР.1.31.2004.00987 (2009). *Measurements of concentration of zinc, cadmium, lead and copper with using a method of inversion voltammetry.* Tomsk, 24 p.
5. ФР.1.39.2007.03222. (2007). *A method of assesment of toxicity of water and water extracts from soils, sewage sediments and wastes on mortality and change of fertility of water fleas.* Moscow: AquaRos, 52 p.

Physical properties of geomaterials

Maghidov S. Kh. Oil and gas extraction and elastic potential of the earth's bowels

Institute of geology DSC RAS salavmag@yandex.ru

Despite the significant volumes of dissolved gases in underground waters there is rapid depletion of them due to the oil- and gas development. It results in significant decrease in the proportion of flowing wells caused by reduction of elastic potential of formations and can refer to significant unaccounted artificial degassing. Man-made change in thermal and pressure conditions in the bowels can involve dangerous geo-ecological consequences and therefore requires further study of the physico-chemical properties of geological materials under high PT conditions in order to predict the possible events and protect the geological environment.

Key words: elastic potential of the bowels, natural gas production, the elastic-and-plastic properties, fluid system, the geological environment, geo-ecological state of the bowels

Reference: Maghidov, S. Kh. (2012), Oil and gas extraction and elastic potential of the earth's bowels, *Vestnik ONZ RAS, 4*

According to estimation of a number of authors (L. M. Zorkin, V. N. Kortsenstein, B. V. Stadnik and other) the volume of dissolved in stratal waters gases in oil and gas basins of the former USSR make up $4.2 \cdot 10^{15}$ m^3. Relevant data are given in the Table 1.

If to comparison these data with contemporary level of natural gas production (2009) in the CIS these recourses should be sufficient for the given territory for 5 thousand years [*Sokolin*, 2010]. The curves of oil and gas output in RF are similar to the curves of total output in the USSR (CIS) and are illustrated by Fig. 1.

There are some correlations between reduction in the elastic potential of the earth's bowels and the level of oil and gas raw materials extraction. As an indicator showing the compressibility properties of the bowels it is convenient to use the data on change in the share of flowing wells when developing the fields. The data for oil and gas industry of USA are given in the Fig.2.

The global volume of dissolved gases for stratal waters of oil and gas basins of the world according to data of the most authors are varied within the limits of 10^{16}–10^{17}m^3. [*Zorkin*, 1989; *Valyaev, 2011a; b*]. I.e. for modern level of gas output its reserves dissolved in underground waters should be sufficient for approximately 15 thousand years.

Table 1. Volumes of dissolved gases in stratal waters of oil and gas structures in the territory of the former USSR [*Zorkin*, 1989]

Geological structure	Volume of dissolved gases, trillions m^3
West European platform	1474.3
Siberian platform	745
East Siberian plate	1000
Scythian and Turanian plates	439
Turanian plate	151
Modern geosynclines and Cenozoic troughs	375.2
Total	4184.5

Fig.1. Oil and gas output in Russian Federation.

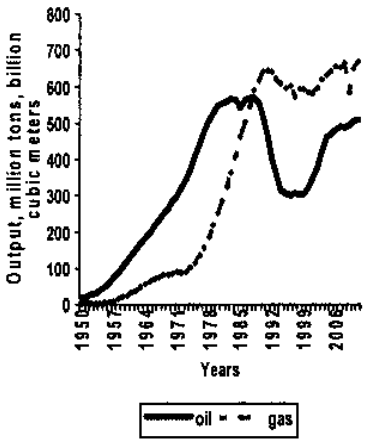

Fig.2. Proportion of flowing wells in the oil industry of the U.S.

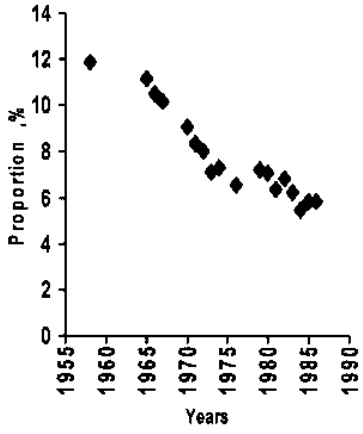

Dashed lines – the calculated values

Fig.3. Operating oil and gas well stock in Russian Federation.

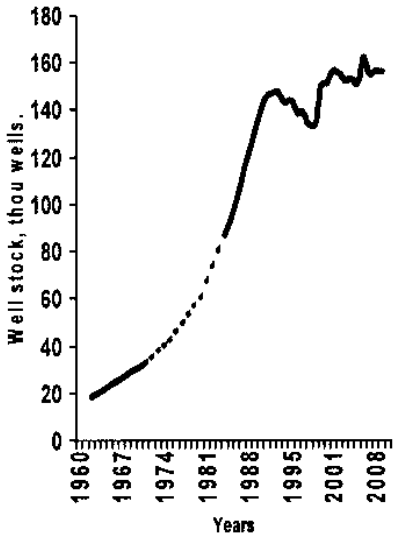

Fig.4. Dynamic of the average density change for oil and gas wells in RF (operating well stock).

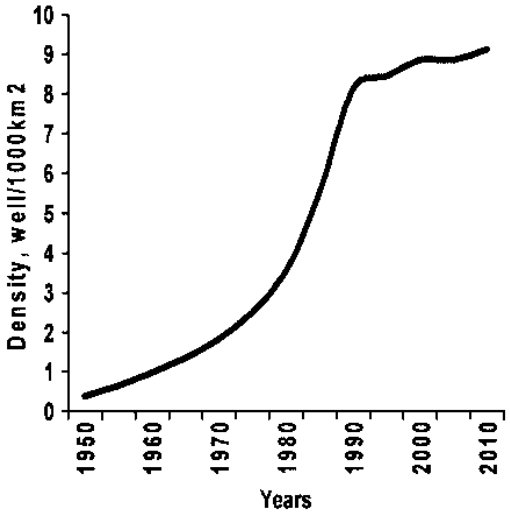

However, nevertheless such enormous reserves the elastic potential of bowels in the territory of RF is already exhausted. The essential reduction of the quote of flowing wells, decreasing their flow rates and increasing of oil watering with the time testifies to it. So, for the past half-century the share of flowing wells in RF is reduced almost by an order, similar decrease have occurred in the countries of CIS as well, it means that compressibility potential has lost significantly in these territories, which occupies 15% of the land. Information about these negative changes there is in the works [*Maghidov*, *2011 a, b*]. In the work [*Maghidov*, *2011b*] the data are given that in the USA, one the largest regions of the world, the quote of flowing wells fell below the threshold of 10% back in the 60s of last century, as evidenced by Fig.2. Russia achieved this only in the beginning of the 90s [*Maghidov*, *2011b*].

At the same time over the past half-century the operating well stock has increased in RF more than by factor 8; the average depth of wells has been increased during this period significantly [*Maghidov*, *2011a*]. The quantitative data on growth of the operating oil and gas well stock are shown in Fig. 3.

It should be noted that the total number of wells several times overpasses the operating well stock in RF therefore the summary density of wells is accordingly higher. In the given work only the density of development wells are taking into account.

Similar situation exists in other countries. As the number of wells the density of wells increases in the territory of individual countries and the world as a whole. Summary qualitative data on wells and their density in RF and in the world were given in [*Maghidov*, 2009] as of 1995. Dynamic of the average density change for oil and gas wells in RF is shown in Fig.4.

Data on changes in the density of wells represented in Fig.4 indicate significant slowing the rates of the density of wells growth last time in the territory of RF.

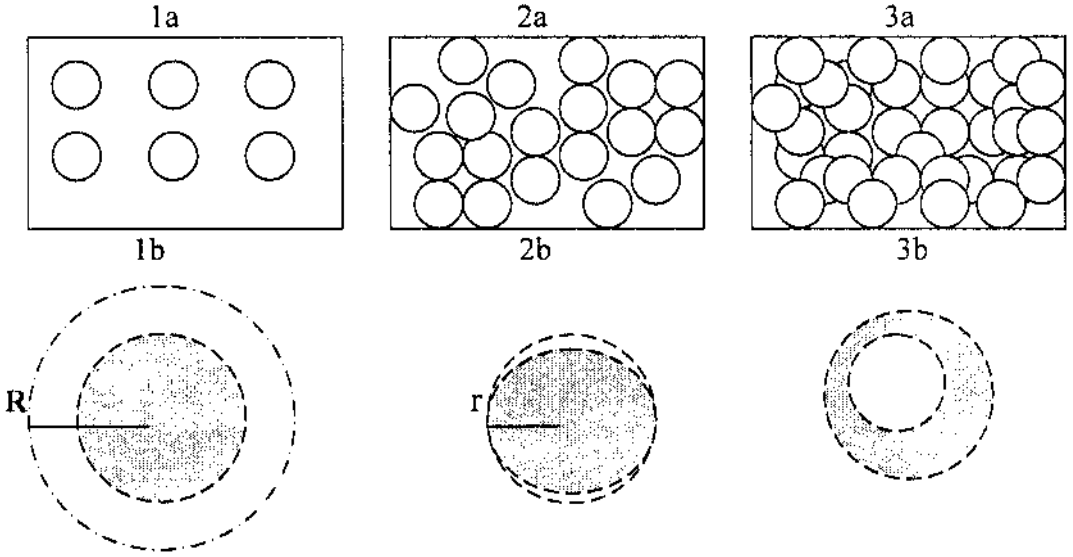

Fig. 5. Schematics of the density of wells spacing in the territory of the region
1. R>r (low density). 2. R=r (critical density). 3. R<r (supercritical density)
R is the average radius corresponding to one well (light area), r – radius of well influence (dark area); **a** is the density of well spacing on the territory; **b** is the zone of influence of an individual well (dark area)

Accordingly the drop in the proportion of flowing wells decreased in oil and gas industry of RF that illustrated by diagrams in the work [*Maghidov*, *2011b*]. As a whole one can speak about existence of inversely proportional relationship between the density of wells and the share of flowing wells. It means that further increasing the number of wells will contribute in even greater defluidization and thus a more rapid depletion of the compressibility potential. Increasing in the well density and their interference are shown schematically in Fig. 5.

Now we are probably in a situation when the density of wells approaches to position 2 (Fig.5) – the critical area where the average radius corresponding to one well became equal to the average radius of wells influence. The basic difficulty is to determine this average radius of influence. Strictly speaking some influence of an individual well or the system of wells to pay horizon can spread for 10 and more kilometers, the data given in the work [*Maghidov*, 2010] indicates to it.

The given above estimations of reserves of dissolved in stratal waters gases probably have been executed for all earth's crust; the mentioned discrepancy then can be explained to some extent. Nevertheless, such rapid changes of the elastic potential of fluidal system can speak about significant unrecorded anthropogenic degassing, and inspire great concern over ecolological condition of the subsurface.

Changes caused by violation of the thermobaric field over large areas can impact to the very course of geodynamic processes. Violation of the natural hydrodynamic and hydrochemical regime as a result of oil and gas production entails not only the occurrence of local man-made anomalies, but forms global anomalies in such large regions as RF and USA. It may indicate that the density of wells is close to the critical point (Fig.5) and the very scales of artificial degassing took invalid dimensions.

Half a century ago academician A. P. Vinogradov noted the leading role of processes of the Earth's degassing in forming not only atmosphere and hydrosphere but geological objects in the bowels of the Earth [*Vinogradov*, 1964]. On opinion of some scientists, the degassing scales not only control the biosphere, but also determine the possibility of continuation of life on the Earth.

Today even registered artificial degassing connected with natural gas production already exceeded by an order the natural level of hydrocarbon degassing. According to the data of the author of [*Valyaev, 2011a*] the global scales of underground hydrocarbon degassing are $2 \cdot 10^{14}$ g/year that are significantly below of annually production of natural gas.

Under these conditions the investigations become vital, allowing to make reasonable predictions of behavior of the global geohydrodynamic system when growing rate of anthropogenic impact to natural fluid systems. It relates, first of all, to study of underground compressibility potential depletion. Studies of influence of changes in the thermobaric conditions to geochemical and geodynamical processes are equally important. In broad terms this requires investigation of theoretical and practical aspects of artificial defluidization of the bowels. Much can be calculated, but the targeted wide-scale studies are needed of geological environment behavior under impact of anthropogenic activity. As a reference one it is necessary to carry out experiments to study in situ the patterns of processes of natural changes in geological environment to have possibility to estimate further the consequences of man-made impact.

The above requires in additional wide complex of investigations of physico-chemical properties of geological materials at high *PT*-conditions as well change of elastic and plastic properties of argillaceous formations, especially pellite fraction when interacting with geofluids.

References:

1. *Waters of oil and gas fields of the USSR* (1989). Ed. L. M. Zorkin, Moscow: Nedra, 110 p. (in Russsian).
2. *Commonwelth of Independent States in 2009* (2010). Ed. V. L. Sokolin, Moscow, 38 p. (in Russsian).
3. Valyaev, B. M. (2011a). Hydrocarbon degassing of the Earth, geotectonics and oil and gas origin, *Degassing of the Earth and genesis of oil and gas fields*. Moscow: Geos, p.17–25 (in russsian).
4. Valyaev, B. M. (2011b). Unconventional resources and hydrocarbon accumulations: features of processes of oil and gas accumulation, *Degassing of the Earth and genesis of oil and gas fields*. Moscow: Geos, 396 p. (in russsian).
5. Maghidov, S. Kh. (2011a). Study of anthropogenic changes of underground geo- hydrosphere for assessment and prediction of geo-environmental hazard, *Vest. Otd. Nauk Zemle*, 3, NZ 6068. doi: 10.2205/2011NZ000198.
6. Maghidov, S. Kh. (2011b). Depletion of elastic energy resources in oil and gas fields of the USSR and RF and change of oil production level, *Degassing of the Earth and genesis of oil and gas fields,* Moscow: Geos, p.490–495 (in russsian).
7. Maghidov, S. Kh. (2009). Wide-scale geochemical and fluido-dynamic "experiment" and its possible consequences in the nearest prospect, *Vest. Otd. Nauk Zemle RAN*, №1.
8. Maghidov, S. Kh. (2010). Anthropogenic impacts in the region of Shamkhal-Bulak gas condensate field and the Daghestan earthquake of 1970, *Monitoring and prediction of natural disasters,* Makhachkala, p.90–94 (in russsian).
9. Vinogradov, A. P.(1964). Gas regime of the Earth *Chemistry of the Earth's crust*. Moscow: Nauka, p. 5–21 (in russsian).

Nikitin S. M., Buyanowa D. S. Mechanisms of destruction rock and solid-phase mass transfer in cracks

Moscow State Mining Universiti, Russia archont@mail.ru

Numerous monitoring effects of mining strikes in underground mines are able to the analysis of the dynamics of intense condition developed methods for kinematic analysis of arrays. The focus of attention paid to the reconstruction of deformations of morfostrukture of surface relief of chips, does not entail an assessment of limit States array. The nonlinear mechanics processes of deterioration are essentially to the analysis of stress intensity factors K_1, K_2, K_3 at the ends of the cracks and as the main criterion was adopted by J-integral Cherepanov-Eselbi-Rice. Under this criterion to the destruction of the kinetic energy to fracture treated with increasing mass transfer characteristics from product fragmentation. Experiments performed to determine crack resistance and specific surface energy of destruction of marble, limestone, granite and serpentinite on a 3-point bending cyclic prismatic designs draw attention to manifestations of solid phase mass transfer for the first time registered, synchronous with growth of cracks. Material emissions occur in the form of shots in connection with movement and zone extended development before the before the destruction of the tip of the cracks, the disclosure of the coast cracks clearly lags behind. The evaluation of the energy balance analysis of crater-like form of destruction around the gas-liquid inclusions in obsidiane on the road cracks, considered as a fundamental tool of destruction phase. Implementation of the latter also explains the transfer of material

beyond any limitations, the experimentally confirmed by acts of the local destruction of rocks, cataclastic current when you reset the load during the test specimens for strength in uniaxial loading.

Keywords: Rock Mechanics, crack, phase-explosion, nonlinear mechanics

Reference: Nikitin, S. M., D. S. Buyanowa (2012), Mechanisms of destruction rock and solid-phase mass transfer in cracks, . *Vestnik ONZ RAN, 4, (doi:)*

Rudakov V.P., Tsyplakov V.V. Fluiddydamic effects in variations of radon seismic noise and telluric carrent fields

O.Y. Schmidt Institute of Physics of the Earth RAS, Moscow

At measurements of the geophysical fields having different origin where unknown effects of fields reaction on the fluiddynamic regimen change of the sedimentary cover in the point of investigations established.

Key words: geostructural elements karst-suffosion processes, fluid- transmission, seismic noise, subsoil radon magnetotelluric current.

Ref: Rudakov, V. P., V. V. Tsyplakov (2012), Fluiddydamic effects in variations of radon seismic noise and telluric carrent fields, *Вестник ОНЗ РАН, 4*,

In the investigations development on studies the effect of different geodeformation processes on the fluid dynamic regimen in the fault geostructural formations of the East European platform in August 2005 we conducted comparative measurements of the emanation (radon) and seismoemission fields variations and variations of magnetotelluric field in the point, located in Nizhny Novgorod oblast. The choice of the area to conduct investigations is related to the fact that the regional structural-tectonic features of the geological environment in the observation point, determining the dynamics of the fluid transportation in tectonically decompressed sediments, are forming by a zone of dynamic influence of regional arcade fault [*Makarov,1996*], bounding the morphostructural complex sedimentary cover neighborhoods of " Holy Lake ", on the south bank of which observations were made. Moreover, in the upper floors of stratigraphic sedimentary complex, presented a power layer of carbonate rocks, overlained by a slight layer of sandy sediments, in point of observation are identical to those which are characterized by intensive development of karst-suffusion processes in Dzerzhinsk [*Natural hazards,2002; Mudler and others, 2004*], representing one of the major geo-ecological problems of the city. Moreover, in the environs of "Holy Lake" karst is also manifested by numerous sinkholes of various sizes and ages, reflecting the permanent nature of modern geodynamic activity in the territory that forms its morphological appearance. Therefore, the choice of place of observation, located at a considerable distance from industrial sites and cities, is exceptional in terms of assessing "natural background" and the possible anomalous effects in the measured parameters of the studied fields.

Monitoring of the subsoil radon concentration variations in the point of observation was carried out using passive (in situ without sampling) continuous measurements using the original sensor installed to a depth of 1 meter. Measurements of seismic noise were carried out using geophones CB-5, buried next to the radon sensor. The measurements of the magnetotelluric field variations were carried out in situ with the help of contour beyond the induction variometer with a diameter of 0.2 m on the inductance 1Gn and the resonant frequency of 5 kHz. Record of information received from the sensors was carried out using a microprocessor 12 bit device "Logger" with a frequency of 1 minute survey. Than, after the transfer of data in computer memory recording the results were averaged in intervals defined in the subsequent analysis of spectral characteristics and interrelation dependencies derived time series.

Fig. 1 shows a comparison of the fragments of continuous recording of the time-series variation of the telluric current subsoil radon and seismic noise envelopes.

Fig. 2 shows the inter-related functions corresponding time-series. Table 1 shows the most representative periods of the harmonic components, selected by the spectral analysis of the temporal realizations.

As can be seen from fig.2, between the time series of subsurface radon and magnetotelluric field current isobserved a significant correlation (R = 0.4) at two-minute delay field magnetotelluric current with respect to variations of the field of radon. This circumstance, in our view, indicates the existence of a common source controlling migration process in an upward fluid flow of radioactive emanations (radon and thoron) and their decay products and the process of forming the components of magnetotelluric variations of current. Such a source, in our opinion, reinforced by the experience of many years research in seismically active regions, is the edge of the capillary fringe above the fluctuating water table, which is sensitive to both the change in pressure in the aquifer, as well as to changes in atmospheric pressure. In addition, the atoms decay of radon, thoron and their decay products alter the conductivity of the capillary moisture, thus changing the magnitude of the electric component of the

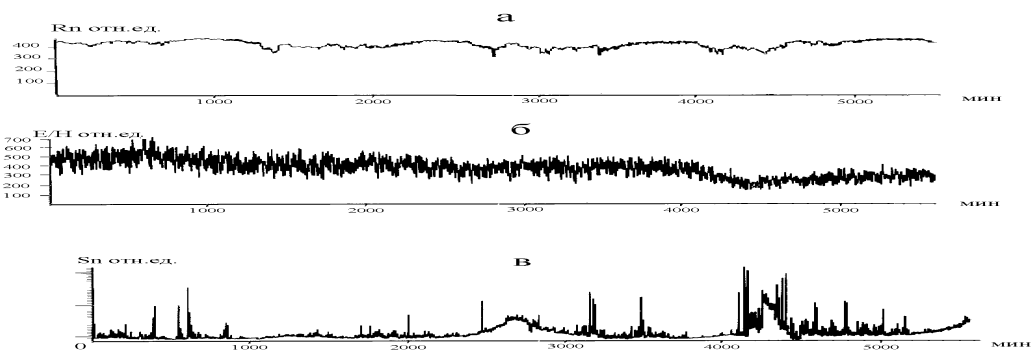

Fig. 1. Time series of variations: a) subsoil radon, b) magneto-telluric current, c) seismic noise in the point of observation. The relative magnitude of measured parameters are given in values of the voltage at the input of the recording device

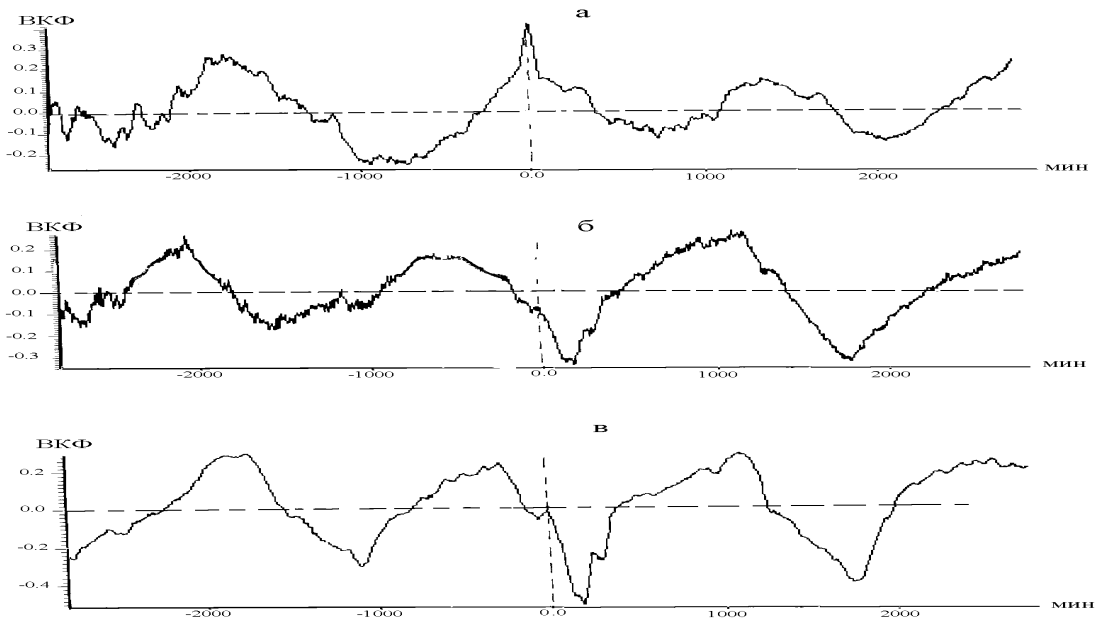

Fig. 2. Interrelation functions of time series: a) variations of radon and magnetotelluric current, b) the variation of magnetotelluric and seismic noise current, c) variations of radon and seismic noise

magnetotelluric current, i.e. its input impedance. Therefore, there is almost synchronous change these parameters – the field of radon and of the magnetotelluric current field.

Meanwhile, a significant negative correlation (R = -0.35) are indicated between the current time series of magnetotelluric current and seismic noise is characterized by the telluric current delay with respect to the noise with an interval of 180 minutes. At the same time, a significant negative correlation (R = -0.46) was observed between the time series of radon and seismic noise with a delay relative to the noise of radon and 180 minutes. Earlier, similar relationship between variations of the emanation fields and variations of the seismic noise was observed by us in Moscow, where the main component of seismic noise is the noise of the city [*Parshikova et al., 2004*]. In this case, despite the absence of an express part of the daily variations in seismic noise (Fig. 1 d), characteristic of the urban environment, all functions of the interrelation of time provided implementations of circadian components, however, stand out.

Therefore, on the basis of received data the mechanism of formation of the relations of cause and effect in the formation of a dynamic component of the upward fluid flow is represented as a process of modulation affecting of the emanations transfer processes, including the process of forming a dynamic component of the magnetotelluric current, by local sources of seismic noise, existing in the geostructural elements of the sedimentary rocks of the "Holy Lake" neighborhoods. Although this view is not undisputed, it still gives some idea of the geological and geophysical processes occurring in the surface layers of the sedimentary cover, confirming the results of spectral analysis below.

Table 1 shows the components of the spectrum interrelation functions shown in Figure 2., which were obtained after removal from spectrum of the daily dominant, allowing in the time series of considered parameters separate a high frequency harmonics, indicating the nonlinear nature of the processes, confirming the presence in the environment local seismic sources.

To reveal more of the fine structure of the interdependence of the investigated time series were calculated by the correlation function of a sliding window width of 1.8% on the value of time realizations and calculate their spectra, the periods are given in Table 2.

Table1. Periods of spectral components interrelation functions of the measured time series of parameters after exclusion of the daily component

R	Ref. spectrum	T	T2(h)	T	T3 (h)	T4	T4(h))	T5	T5 (h)	T6	T6(h))
	Radon/current	12	12.4	6	6.8	4	4.9	3	3.9	2	2.8
C	Current/seism	1	11.4	6	6.8	4	4.9	3	3.9	2	2.8
S	Seism/radon	1	12.4	6	6.8	4	4.9	4	4.0	3	3.3

Table 2. Periods of the correlation functions spectra of the sliding time series

Re	Ref. spectrum	T1	T1(h)	T	T2(h)	T	T3(h)	T	T4(h)	T	T5 (h)	T	T6(h)
	Radon/current	2	27.3		12.4		9.1		4.9		3.25		2.6
	Current/seism		27.3		13.7	5	5.5	4	4.3		3.25		2.8
Se	Seism/radon		22.8		8.0		5.5		4.0		2.8		2.6

As follows from the data, with the overall positive correlation between these time series of radon and magnetotelluric current relationship between them is of alternating sign. The values of the correlation function reaches almost one hundred per cent level as for direct, so for inverse relationship of the parameters. A similar pattern (for a total of negative correlation) observed for the time series of telluric currents and seismic noise, as well as for time series of radon and seismic noise.

The periods of variations of components of investigated time series, are listed in Table 2, do not always coincide with periods of harmonics in Table 1, which apparently indicates a more diverse combination of factors determining the dynamics of fluid transportation in the point of measurements. However, the interrelation relationship between the variation of the field of radon and the field of seismic noise in the point of observation, as well as correlated with the field of radon field in one of the components of the spectrum of magnetotelluric currents is significant. However, in contrast to that observed previously in Moscow [*Parshikova, et al, 2004*], this dependence can not be explained by variations in the urban seismic noise acting on the dynamics of the ascending fluid flows, as the nearest of the "Holy Lake" town Murom is located about 30 kilometers on the opposite bank of the river Oka, absorbing the noise of the city. Interecorrelation connection between the fields of radon and seismic noise, as well as between the fields of seismic noise and telluric current is an alternating character, changing from wavy significant positive to significant negative values. Such variation of the correlation coefficients between the fields of seismic noise and emanations of radon and magnetotelluric current can be attributed to the nature of the changes flyuid transportation under of the stress-strain state of rocks changes in the structural-tectonic formation in the area of dynamic influence of which is the point of observation. The influence of the above named regional arcade structural-tectonic formation on a nature of the sedimentary rocks anisotropy permeability the environs of the "Holy Lake" and, respectively, on the dynamics of the rising fluidtransportation, studied by us via the radial-azimuth surveys, does not have an explicit nature. This type of the anisotropy permeability formation of the sedimentary cover was noted in the area of the annular geostructural formation [*Kozlova and others, 1999*], when deformation of the sedimentary cover rocks have no pronounced one or two-way orientation. At the same time, the spectral analysis of time series (see table) shows the effect of the tidal deformations on the dynamics of the vertical components of fluidtransportation that is manifested by the presence of the time series of the periodic spectral components of the diurnal and semidiurnal harmonics.

Thus, the existing preconditions for the establishment in the studied fields the more fine structure of the interaction of hydro and physic-chemical processes allow us to hope that getting a longer time series will allow implementations to identify those features of the formation vertically upward fluid flow, which occur under the influence of the processes that accelerate the development of karst-suffusion phenomena of one of the major geo-ecological problems of the region. In this case, the results of complex monitoring of the fluid dynamic processes using measurements of variations of emanation and seismoemission fields, together with the registration of high-frequency component magnetotelluric currents, carried out in geodynamic active area of the Nizhny Novgorod region, showed that on the basis of the data, one can create an effective set of monitoring of the geological environment and development of geo-ecological processes.

References:

1. Kozlova, N. S.,V. P. Rudakov, V. N. Shuleikin, G. I. Voitov (1999). Emanation and electrical effects in the subsoils atmosphere above Kaluga impact ring structure, *Russian Journal of Earth Sciences*, v. 1, N 6, p. 503–510 (in Russian).
2. Makarov, V. I. (1996). On the regional characteristics of the modern geodynamics of the platform areas in connection with evaluation of their tectonic activity, *Bowels of the Volga and the Caspian Sea,* issue 13 (Special), November, p. 53–60 (in Russian).
3. Mudler, E., V. I. Osipov, V. M. Kutepov et al (2004) To the estimation of danger and risk in urban and industrial areas on the example of karst ground control stations in Moscow and in Dzerzhinsk, *Proceedings of International Symposium: Karst - the twenty-first century, The theoretical and practical importance, May 25-30, 2004, Perm., p. 24–36.*
4. Natural hazards in Russia. Exogenous geological hazards (2002), Ed. V.I.Osipov et al., M.: Crook, 345 (in Russian).
5. Parshikova, N. G., V. P. Rudakov, V. V. Tsyplakov (2004). Modulation of fluid flows of the faulting geological structures by the urban seismic noise (for example, variations of radon emanation and hydrogen in Moscow.), *Geochemistry,* N3. p.332–336 (in Russian).

Rudakov V.P. Factors of global fluid transportation and catastrophyc earthquakes

O.Y. Schmidt Institute of Physics of the Earth RAS, Moscow
rudak@mail.ru

On the base of previously reserved a scheme of the geodeformation pulsation centers global displacements was their connection to the catastrophic earthquakes of the last years shown.

Key words: fluid dynamics, monitoring, geodeformation waves, geodeformation pulsation centers, earthquakes

Citation: Rudakov, V. P. (2012), Factors of global fluidtransportation and catastrophyc eartquakes, *Vestn. Otd. nauk Zemle, 4*

Investigating geodeformation processes that appear in the variations of fluiddynamic (primarily emanation) fields of the earth's crust fault geostructural formations of the geosinclinal (seismic) and platform regions of the former USSR, we have identified several patterns of spatial and temporal distribution of geodynamic events, showing their connection with processes of the lithosphere's self-organization, accompanying changes in rotational regimes of the Planet [*Rudakov, 2004; Rudakov, 2009*]. According to the analysis of dynamics of these patterns manifestation across the globe a map diagram (Fig. 1) was made of the global distribution centers of the geodeformation pulsation (GDPC) of the lithosphere. These centers represent a field of "interference" (combination of extremes) latitudinal and longitudinal wave components of geodeformation wave of seasonal (annual) periodicity. In this case, for graphic constructions have been used empirically received data on the rate of migration of seasonal geodeformation wave fronts in the latitude (7 km/day) and longitude (28 km/day)

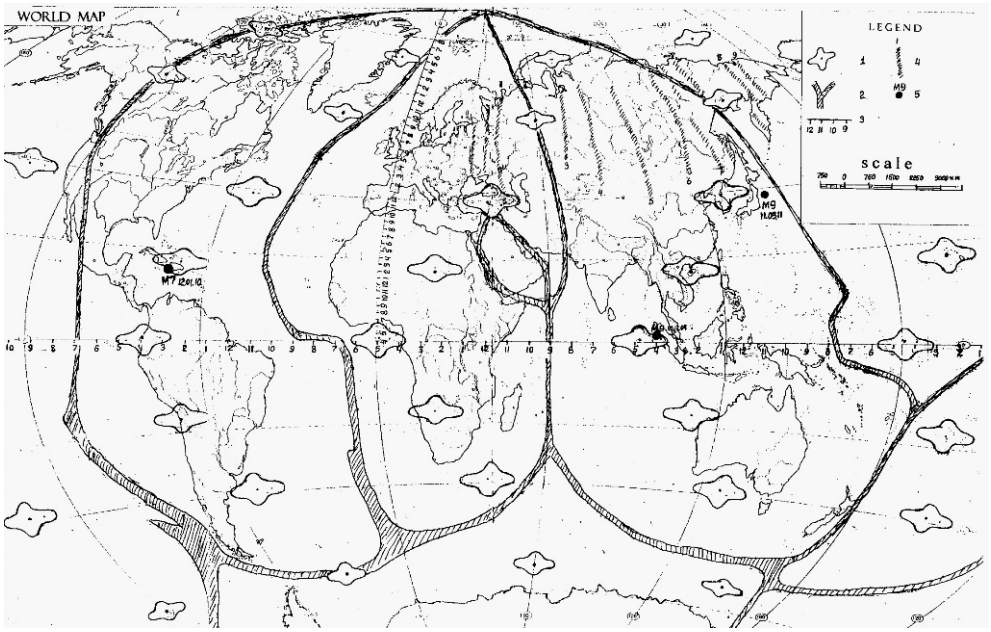

Fig. 1. The scheme of the global placement of geodeformation pulsation centers of the earth's crust. In the scheme are also plotted: 2 - main trunks of the world rift system, 3 - time scales of migration fronts of seasonal geodeformation wave in the latitudinal and longitudinal directions, 4 - the main faults of meridional system of the former USSR [according to *Sivorotkin, 2002*]. The numbering corresponds to the meridional lineaments shown in [*Sivorotkin, 2002*]. Button (5) corresponds to the location of the catastrophic earthquake in Sumatra, Haiti, and in Japan.

directions with reference of the extrema points of this wave movement to specific coordinates, i.e. to those in which a long-term monitoring of the geodeformation processes was made.

A characteristic feature of the seasonal geodeformation wave is exposure its amplitude (at average values of the order of 0. $3x10^{-6}$ [*Nersesov et al, 1985*] by the modulating influence of the long-geodeformation waves, as result of which the amplitude can reach critical levels (about 10^{-4}). Exceeding these values is accompanied, as a rule, by emission of seismic or volcanic (in respective regions) energy and other geodynamic phenomena [*Rudakov, 2004; Rudakov, 2009; Zhdanova, Rudakov, 1993; Rudakov, 1993*].

At the same time, the seasonal geodeformation wave affecting the amplitude and phase parameters of wave geodeformation processes of intra year periodicity, determines the dynamics of the more higher-frequency interval of the spectrum of the geodeformation "vibro" affect on the fluid system of the underground hydrosphere. This allows us to consider GDPS depicted on the scheme as local sources of rhythmic geodeformation impact on the formation fluids. The range of this influence extends from the vibrations of intra year periodicity to diurnal frequency components that contribute to directed transport ("pumping") of fluids of the fault structures in the latitudinal and longitudinal directions.

As follows from the received scheme GDPC are located (mostly) over the geodynamically active points of the Planet, superimposed on the overall configuration of the major continental and intercontinental paleorifts, continental paleooutskirts and marginal basins of the crust. Moreover, they (the centers) coincide or are close to many well-known hydrocarbon accumulations provinces both in Russia and abroad. The latter suggests that in the formation of oil and gas accumulations of the sedimentary cover and in the regularities of distribution in the crust oil and gas accumulations geodeformation factor determined by the rhythmic action centers on the lithosphere geodeformation pulsation, is no less important than factors of geological and geochemical origin. It is also clear that due to geodeformation factor affecting the change of the fluidtransportation regimes in the crust, are created conditions conducive to the development of relevant geological and geochemical conditions and thermal regime of the formation of hydrocarbon deposits.

Analysis of the space-time location on the world map of the geodeformation pulsation centers of the earth's crust in the precondition of their connection with the provinces of hydrocarbon accumulations, shows not only the affinity of both to the active geodynamic structures of the Earth's crust, but also direct participation of GDPC in the processes of the hydrocarbon accumulations formation. This participation is determined, above all, by the formation of excess pressure in the fluid-saturated layers, contributing to directed transport ("pumping") in them oil and gas components in systems of meridional faults in the northern direction for northern hemisphere and in the south direction for the south hemisphere.

The last circumstance is a prerequisite for the formation of huge accumulations of hydrocarbons in the polar systems of rifting. The assumption, apparently, is also valid for faults trending east-west, but in this system of lineaments crustal fluid migration is carried out exclusively in a western direction, in accordance with the direction of movement of the fronts of longitudinal component of the seasonal geodeformation wave.

All this creates conditions for the strategy planning of exploration studies based on tracing the known and anticipated zones over rift geostructural formations, superposed in space with the location of the geodeformation pulsation centers of the earth's crust, and the search within the zones of their dynamic influence of the structural "traps" that provide long-term (at geological standards) preservation of hydrocarbon accumulations.

At the same time, ability to recover on the basis of a retrospective analysis of the velocity regimes of the planet at various epochs of its geological history, the system allows you to recreate over rift paleostructural formations that are favorable for the formation of petroleum accumulations. Thus, for the modern earth's rotational regimen, which determines the position of the continental

rift controlling structures and placement of the geodeformation pulsation centers of the earth's crust in the territory of the Russia the perspective of not studied areas are the Verkhoyansk mountain range and the shelf of the East Siberian Sea. Moreover, the dimensions of hydrocarbon accumulations in these areas, probably comparable to the size of oil and gas potential of the West Siberian petroleum province and the Kara Sea shelf, which is consistent with the forecasts of Petroleum Geologists, classifying the named territory as a potentially oil and gas basins [Kleshchev and Shein, 2004].

Besides that the selected "nodes" of geodeformation pulsation of the earth crust coincide with the centers of modern geodynamic activity of the Earth, are repeated in the general configuration the contours of the main trunks of the planet meridianal rift system [*Sivorotkin, 2002*], and superimposed on the area of the formed oil and gas provinces. Their involvement in the formation of hydrocarbon accumulations in the areas of active tectonic destruction of the earth's crust causes provocation of the most catastrophic seismic events. Among the most famous in the last century examples of this symbiosis are Gazly earthquake in 1984, and Neftegorsk earthquake in 1995, and from classical occurred recently are earthquakes near Sumatra December 26, 2004 and March 28, 2005, reached the level of seismic energy is almost nine ball mark on the Richter scale, as well as in Haiti January 12, 2010 and in Japan March 11, 2011.

As can be seen from the figure, the catastrophic earthquakes in Sumatra realized within our dedicated center of geodeformation pulsations, which not only is in the zone of active subduction processes that are formed the morphology of the mountain massif of Sumatra and its vicinity, but also "mark" it (mountain massif), oil and gas capacity (Oil and gas capacity, 1978). So, for the formation of gigantic hydrocarbon accumulations on Sumatra and its vicinity existed geostructural, geochemical, and geodynamic conditions typical for oil and gas basins.

Thus, the analysis results of the study of the geodeformation wave processes dynamics in the geosynclinal and platform regions for determine their involvement in the development of catastrophic geodynamic phenomena allowed to draw a picture of the global distribution of points of the geodeformation pulsation of the earth's crust, formed by processes of rhythmic changes in Earth's rotational speed. It is shown the involvement of these points at the fluid transportation regimes formation and rhythms degassing the Earth's crust degassing, at the formation of structural-tectonic elements and at the formation of minerals of hydrocarbon origin. Confirmed so, that the basis of the nature of catastrophic seismic events is the relationship of areas of formation of hydrocarbon accumulations with areas of contemporary geodynamic activity.

References:

1. Kleshchev, K. A.,V. S. Shein (2004). Plitotektonic models of the oil and gas basins of Russia, *Oil and gas geology,* N 1, p. 23–40 (in Russian).
2. Nersesov, I. L., B. G. Rulev, L. Bokanenko et al (1985). Seasonal variations of several seismic and deformation parameters in the Garm polygon, *Dokl. RAS,* v. 282, N 5, p. 1086–1089 (in Russian).
3. Oil and gas capacity and global tectonics (1978). Transl. from English under edition of S.P.Maksimov M.: Nedra. 237 p. (in Russian)
4. Rudakov, V. P. (1993). On the role of geomovements of the wave structure in the activation of geodynamic processes in aseismic regions (on example of geodynamic phenomena of the Russian Platform). *Dokl. RAS*, v. 332, N 4, p. 509–-511 (in Russian).
5. Rudakov, V. P. (2004). Geodeformation waves in the variations of the fluiddynamic and seismic regimes of geosynclinal and platform areas. *In col.: Studies in geophysics: the 75th anniversary of the Joint Institute for Physics of the Earth,* M.: IPE RAS, p. 119–122 (in Russian).
6. Rudakov, V. P. (2009). Emanation monitoring of the geoenvironments and processes. Moscow: Scientific World, 176 p. (in Russian)
7. Sivorotkin, V. L. (2002). Deep degassing of the Earth and global catastrophes. M.: OOO "Geoinformtcenter." 255 p. (in Russian)
8. Zhdanova, E. J., V. P. Rudakov (1993). On the role of the geomovements of the wave structure in the preparation of volcanic eruptions (on example of northern group of volcanoes of Kamchatka), *Dokl. RAS,* v. 329, N. 1, p. 22–24. (in Russian)

Vitovtova[1] V. M., Shmonov[1] V. M., Zharikov[2] A. V. Hydraulic radius and mole surface of the fluid in the rocks of the earth's crust

[1]Institute of Experimental Mineralogy, RAS, Chernogolovka
[2]IGEM RAS

Structural characteristics of rocks define dynamics of movement of transcrust fluids, and also a contribution of surface energy to thermodynamic properties of fluids in a nanopores. In the conditions of interaction crust solution – rock substantially is defined by properties of an interface of phases. We by a filtration of argon experimentally determined absolute permeability, k^o (m^2), and hydraulic radiuses of a pore of rocks of Rh = Vφ/Aφ, where Vφ - volume of a time, Aφ - a surface of a pore are calculated. Trends of hydraulic radius of a pore of rocks in a continental crust for temperature gradients 9, 15 and 26°C /km are constructed. According to these data effective radiuses of a pore and a specific surface of rocks are calculated at high temperatures and pressure. It is important that value ΔG_f a fluid doesn't depend on granularity of rocks and is defined only by the size of microcracks. Appreciable effect (4 kJ/mol) at interaction quartz – water at temperatures 300 – 600°C and pressure 50 and the 100th MPa it is possible to expect in microcracks in the size of 70-20 nanometers and less.

Zharikov A.V. [1,2], Velichkin[1] V. I., Vitovtova[2] V. M., Malkovsky[1] V.I., Shmonov[2] V.M. Experimental study of crystalline rock filtration properties: implications for underground radioactive waste disposal

[1]Institute of Geology of Ore Deposits, Petrography, Mineralogy and Geochemistry, RAS, Moscow, Russia *vil@igem.ru*
[2]Institute of Experimental Mineralogy, Russian Academy of Sciences, Chernogolovka, Russia

The results of transport properties of tight rocks studies, their interpretation and use for search of the area for safe underground deposition or reposition of HLW and SNF on the basis of the data of physical and numerical experiments were considered. The rock samples collected from the sites of probable location of HLW and SNF depositories or repositories: metavolcanites from the area of PA Mayak. and granitoids from the Krasnoyarsk MCC zone were used for the laboratory study. On the basis of the comparative analysis of the experimental data and the results of microstructure studies the main factors controlling rock transport properties were

found. A forecast of permeability changes under heating due to HLW heat-generation was done. It was considered how to determine intact rock thicknesses enough for safe location of HLW depositories using the results of physical experiments as input data for a numerical one.

Key words: rock porosity and permeability, numerical and physical simulation, well HLW depositories

Ref: Zharikov6 A. V., V. I. Velichkin, V. M. Vitovtova, V. I. Malkovsky, V. M. Shmonov (2012), Experimental study of crystalline rock filtration properties: implications for underground radioactive waste disposal, *Вестник ОНЗ РАН, 4*, (doi: -)

Main requirement for the area selected for location of underground depositories or repositories of HLW or SNF is to minimize the risk of radionuclide escape with underground water to the biosphere. So, an importance of studies of rock transport properties is evident. First of all it concerns rock permeability which is one of the main factors governing dynamics of natural and technogenic fluids flow in the geologic media. Permeability values for tight rocks occurring near the HLW and SNF depositories or repositories are usually very small so their determination is strongly difficult. Therefore the authors developed a special technique for permeability laboratory studies taking into account the peculiarities of gas filtration through tight rocks. Permeability determinations are carried out with respect to changes in filtrating gas properties due to temperature and pressure effects. That allows to perform the measurements with high accuracy within wide range of values (10^{-22}–10^{-15} m^2) at normal and high *PT*-parameters as well. The data obtained in a single test are enough to determine both the values of sample permeability and Klinkenberg factor, characterizing pore shape. Against the conventional methods the measurement accuracy and work content are improved and recording of experiment parameters is simplified.

The studies of transport properties on the samples of the main rock types from the areas of probable location of HLW and SNF depositories or repositories: metavolcanites from the area of PA Mayak (Sothern Ural) and granitoids from the Krasnoyarsk MCC zone (Yeniseian ridge) were carried out with use of the new technique (fig. 1–4).

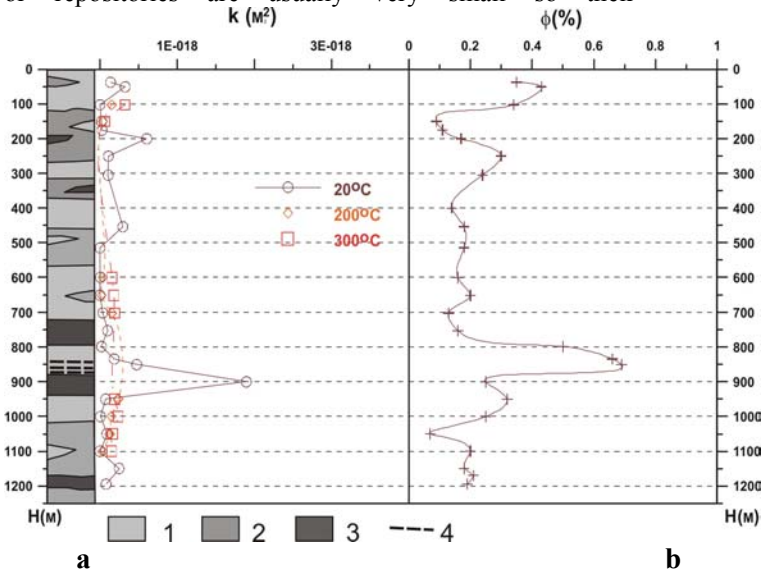

Fig. 1. Permeability (a) and porosity (b) of the samples from the well 8001 and 8002 of Mars-2 site, PA Mayak
1 – tuff, tuff lava; 2 – lava-breccia, 3 – porhyritic andesite-basalt, 4 – schistose rock.

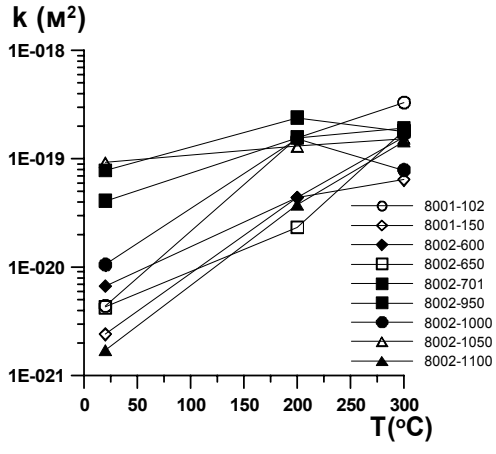

Fig. 2. Temperature dependencies of permeability for the samples from the well 8001 and 8002 of Mars-2 site, PA Mayak. P_{eff}= const = 25 MPa.

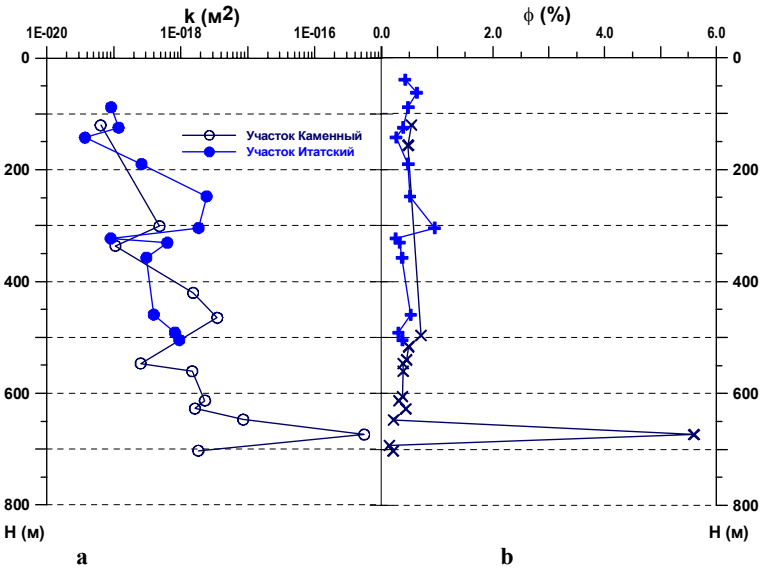

Fig. 3. Permeability (a) and porosity (b) of the samples from the well 1I-500 and 1K-700 drilled in the the Itatsky and Kamenny sites, Krasnoyarsky MCC.

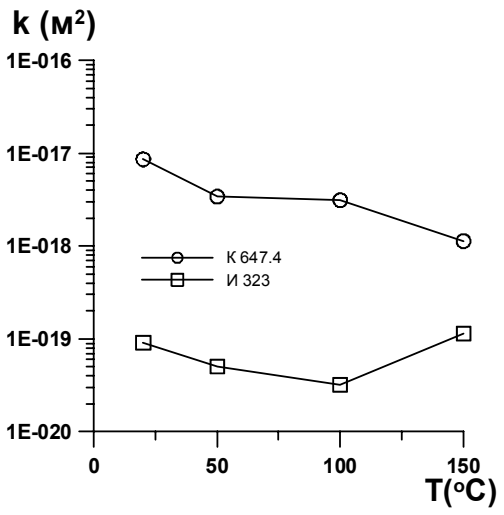

Fig. 4. Temperature dependencies of permeability for the samples from Nizhnekansky massive. P_{eff}= const = 25 MPa.

The results obtained show that beyond the dislocations zones metavolcanites have low values of porosity and permeability. Porosity of the samples varies from 0.07 to 0.69 %, the mean value is 0.26 %. Most of the studied samples also show very low permeability: its values for 17 of 27 samples does not exceed 10^{-19} m^2, mean value is $1.92 \cdot 10^{-19}$ m^2. It is significant that the background permeability values, even taking into account their rise with heating, are considerably lower than that obtained for the samples collected in the schistosity zone under ambient conditions. So, an occurrence of the families of microcracks related to the rock structure, in this case to rock schistosity, is more dangerous factor reducing insulating properties of the rocks of HLW near field than their thermal decompaction.

Permeability values of granitoid samples are also quit low: 0.14 – 0.95 %. (fig. 2. b). Mean values for the site are close: 0.44 % for Itatsky site and 0.37 % for Kamenny one, for both sites – 0.41 %.

Permeability values for most of studied granitoid samples varies from $3.71 \cdot 10^{-20}$ to $8.59 \cdot 10^{-18}$ m^2. Mean value for both sites is $1.30 \cdot 10^{-18}$ m^2. Comparison of the data obtained for the Itatsky and Kamenny sites shows that mean permeability value for first one is three times higher ($1.92 \cdot 10^{-19}$ m^2) than mean permeability of the samples collected from the site Mars-2, PA Mayak. Mean permeability of the samples from the Kamenny is much more higher: by one decimal order ($1.98 \cdot 10^{-18}$ m^2), significant parameter variations are also proper for this site. The trends of permeability increase with depth are typical for both wells (fig. 3a).

So, the mean porosity values for metavolcanites from the Mars-2 site and granidoids from the the Itatsky and Kamenny sites are very close (the difference is only ~ 0.1 %). At the same time mean permeability of granitoids is significantly (one decimal order) higher then of metavolcanites. In [*Petrov et al.,* 2005 a, b] it were shown than during the geological history metavolcanites and granitoids both were exposed to numerous alterations, which frequently lead to second porosity initiation. However higher degree of such alterations is proper to granitoids. The results of microstructure studies reviled that permeability of tight, low porous rock is caused by microcracks [*Zharikov et al.,* 1993]. Microcrack density in granitoids which refer to britle low-rigid type of petrophysical media is significantly higher then in metavolcanites of viscous rigid type [*Laverov et al.,* 2001, *Starostin*, 1988]. As a result mean permeability in granitods is significantly higher then in metavolcanites. However such permeability values are low enough to believe both considered types of rocks as safe media for location of HLW-SFN repositories or depositories if they will be placed in blocks of intact rocks which thickness will be enough.

Permeability behavior under heating (fig. 2, 4) is also controlled by rock microstructure effect. In the initial samples of metavolcanites microcrack density is not high. As a result generation of new microcraks located to mineral boundaries leads to rock permeability increase. In contrast, there are many microcrack of significant length and apertures in the granitoid initial samples. Such microcracks are not stables, so heating firstly may lead to permeability decrease. Subsequent temperature increase may lead permeability decrease within whole temperature range, or inversions on temperature permeability trends may appear: permeability decrease may be changed by parameter increase. It should be noted that even under conditions when parameter values are minimal and close to ones proper to matrix rock permeability in anisotropic rocks survive stables fluid paths at microscale: through oriented mickrocracks along rock schistosity.

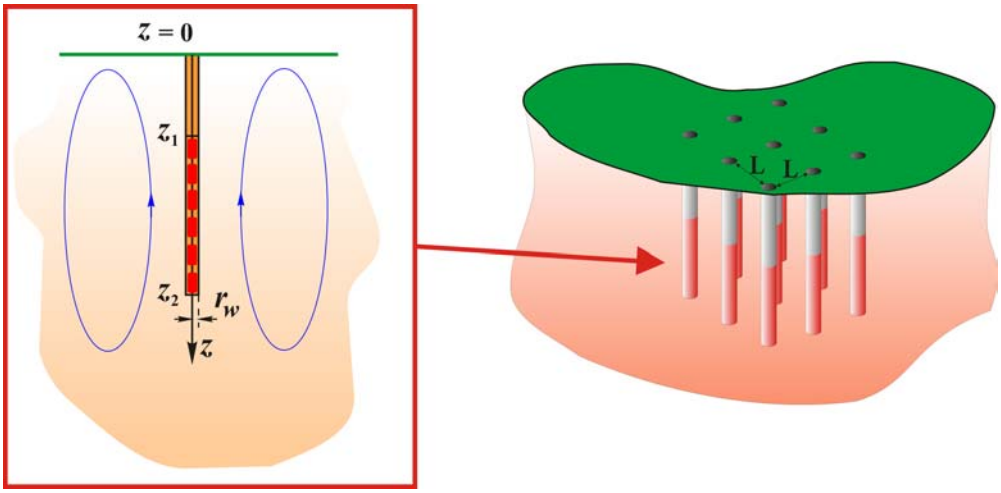

a **b**

Fig.5. The models of well HLW repositories presented by a single well (a) and a cluster of wells (b).

In order to determine the dimensions of intact rock blocks which insure safe HLW and SNF disposal numerical simulation of free thermal convection of underground water arising in the rock massive where a repository is located was carried out. Theoretical basis of the used technique was described in details in [*Malkovsky et al.,* 1998], where a model of repository presented by a single vertical well which bottom part is loaded by the containers with heat-generating HLW (fig. 5 a) was considered. The object of simulation was to estimate the transport of the most dangerous radionuclide - ^{90}Sr by ground water from the repository to biosphere. ^{90}Sr concentration in near surface water was calculated with respect to repository depth, its shape, porosity and permeability of host rocks, thermophysical properties of rocks and water and HLW heat-generation. Such depth (a distance between earth surface and loaded well part – z_1,, see fig 5 a) of HLW well repository was classified as safe if ^{90}Sr concentration in near surface waters does not

exceed its maximum permissible concentration. Key parameters of underground media were determined using the values characterizing low fractured crystalline rocks which compose the sections of Itatsky and Kamenny sites of Nizhnekansky massive [*Petrov et al.,* 2005 a]. So, the results of physical modeling were used as input data for numerical simulation. Computer simulation allowed also to determine the horizontal extent of intact rock blocks for safe HLW disposal [*Malkovsky & Pek,* 2007]. The estimations were based on the simulation of the radionulide transport by thermal convection in cases of single well and a cluster of wells loaded by waste in their bottom parts with respect of HLW and rock physical properties as well . Thereby not only the horizontal extent of intact rock block in case of single well but the distance between the wells in case of cluster of wells were determined (*L*, see fig. 5 b).

Summary

The results of transport properties of tight rocks studies, their interpretation and use for search of the area for safe underground deposition or reposition of HLW and SNF on the basis of the data of physical and numerical experiments were considered. The rock samples collected from the sites of probable location of HLW and SNF depositories or repositories: metavolcanites from the area of PA Mayak. and granitoids from the Krasnoyarsk MCC zone were used for the laboratory study. On the basis of the comparative analysis of the experimental data and the results of microstructure studies the main factors controlling rock transport properties were found. A forecast of permeability changes under heating due to HLW heat-generation was done. Use of the results of physical experiments as input data for numerical one allowed to determine intact rock thicknesses which are enough for safe location of HLW depositories.

The work is supported by RFBR (grant # 11-05-00778) and by RAS (Programs 4 and 8).

References:

1. Laverov, N. P., V. I. Velichkin, B. I. Omel'yanenko (2001). Insulative Properties of Crystalline Rocks: On the Problem of High-Level Radioactive Waste Disposal, *Geology of Ore Deposits*, v. 43, no. 1, pp. 4–18.
2. Malkovsky, V. I., A. A. Pek (2007). Estimation of Loading Density of Underground Well Repositories for Solid High-Level Radioactive Wastes, *Geology of Ore Deposits*, v. 49, no. 3, pp. 194–200.
3. Malkovsky, V. I., A. A. Pek, C. F. Tsang (1998). A new formulation of convective transfer for simulation of mass transport with large concentration variations, *Proc. 4th Int. Conf. "IAMG'98" V.1. - Napoli: De Frede Editore*, pp. 304–308.
4. Malkovsky, V. I., A. V. Zharikov, V. M. Shmonov (2009). New Methods for Measuring the Permeability of Rock Samples for a Single-Phase Fluid, *Izvestiya, Physics of the Solid Earth*, v. 45, no. 2, pp. 89–100.
5. Petrov, V. A., V. V. Poluektov, A. V. Zharikov, et al. (2005a). Microstructure, filtration, elastic and thermal properties of granite rock samples: implication for HLW disposal, *Petrophysical properties of crystalline rocks, Geological Society of London, Special publications, Ed. by Harvey P.K., Brewer T.S., Pezard P.A. & Petrov V.A.,* v. 240, pp. 237–253.
6. Petrov, V. A., V. V. Poluektov, A. V. Zharikov, et al. (2005b). Deformation of metavolcanics in the Karachay Lake area, Southern Urals: petrophysical and mineral-chemical aspects, *Petrophysical properties of crystalline rocks, Geological Society of London, Special publications, Ed. by Harvey P.K., Brewer T.S., Pezard P.A. & Petrov V.A.,* v. 240, pp. 307–321.
7. Starostin, V. I. (1988). *Paleotektonicheskie rezhimy i mekhanizmy formirovaniya struktur rudnykh mestorozhdenii* (Paleotectonic Regimes and Mechanisms of the Ore Deposit Structure Formation), Moscow: Nedra.
8. Zharikov, A. V., V. M. Vitovtova, V. M. Shmonov, A.A. Grafchikov (2003). Permeability of the rocks from the Kola superdeep borehole at high temperature and pressure: implication to fluid dynamics in the continental crust, *Tectonophysics*, v. 370, no. 1-4, pp. 177–191.